VIBRATION OF TUBE BANKS DUE TO CROSS FLOW AND COMBINED CROSS – AXIAL FLOW BY FEM

By

R. SELVA KUMARESAN

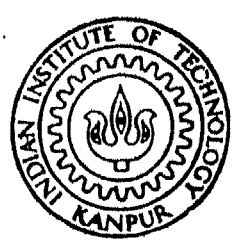

DEPARTMENT OF MECHANICAL ENGINEERING

INDIAN INSTITUTE OF TECHNOLOGY, KANPUR

OCTOBER, 1988

VIBRATION OF TUBE BANKS DUE TO CROSS FLOW AND COMBINED CROSS – AXIAL FLOW BY FEM

A Thesis Submitted
In Partial Fulfilment of the Requirements
for the Degree of
MASTER OF TECHNOLOGY

By
R. SELVA KUMARESAN

to the
DEPARTMENT OF MECHANICAL ENGINEERING
INDIAN INSTITUTE OF TECHNOLOGY, KANPUR
OCTOBER, 1988

CERTIFICATE

This is to certify that the work entitled, "Vibration of Tube Banks due to Cross Flow and Combined Cross-Axial Flow by FEM", by R.SELVA KUMARESAN has been carried out under our supervision and has not been submitted elsewhere for a degree.

(Dr. B.L. DHOOPAR)
Professor
Department of Mechanical Engg.
I.I.T. Kanpur-208016

(Dr. BHUPINDER PAL SINGH)
Assistant Professor
Department of Mechanical Engg
I.I.T. Kanpur-208016

October, 1988

ACKNOWLEDGEMENTS

I wish to express my sincere thanks to Dr. B.L. Dhoopar and Dr. B.P. Singh for their constant encouragement, comments and valuable guidance at various stages of my thesis work. I also thank all my friends for their support and company.

Thanks also to Mr. H.V.C. Srivastava for his patient and accurate typing.

R. Selva Kumaresan

CONTENTS

LIST OF FIGURES

LIST OF SYMBOLS

c_i	Structural damping coefficient for tube i in X direction
e_i	Structural damping coefficient for tube i in Y direction
E_iI_i	Flexural rigidity of tube i
f	Fundamental natural frequency of tube in vacuum (Hz)
f_i	Cross flow fluid force per unit length acting on tube i in X direction
f_s	Vortex shedding frequency (Hz)
g_i	Cross flow fluid force per unit length acting on tube i in Y direction
G/R	Gap to radius ratio
h	Length of the finite element
Im(Ω)	Imaginary part of dimensionless frequency
j,k	Node numbers associated with e^{th} element
K	Number of tubes in the tube bank
L	Tube length
m_a	Mass of the internal fluid per unit length
m_i	Mass per unit length of tube i
Re	Reynolds number
R_i	Outside radius of tube i
Re(Ω)	Real part of dimensionless frequency
S	Strouhal number
t	Time
u_i	Displacement of tube i in X direction

U_o	Cross flow velocity
U_r	Reduced cross flow velocity
U_r^*	Critical reduced cross flow velocity
v_i	Displacement of tube i in Y direction
V	Dimensionless axial internal flow velocity
V_a	Axial internal flow velocity
V^*	Critical dimensionless axial internal flow velocity
X	Coordinate in the drag direction
Y	Coordinate in the lift direction
Z	Coordinate in the axial direction
α_i	X component of steady state fluid force coefficient
β_i	Y component of steady state fluid force coefficient
$\alpha_{ij}, \sigma_{ij}, \tau_{ij}, \beta_{ij}$	Added mass coefficients
$\alpha'_{ij}, \sigma'_{ij}, \tau'_{ij}, \beta'_{ij}$	Fluid damping coefficients
$\alpha''_{ij}, \sigma''_{ij}, \tau''_{ij}, \beta''_{ij}$	Fluid-elastic stiffness coefficients
β	Inside fluid mass ratio
ν	Outside fluid mass ratio
τ	Damping ratio
δ_m	Mass-damping parameter
δ_{ij}	Kronecker delta

ρ	Cross flow fluid density
λ	Eigen value
$\theta_i \Big\vert_j$	$\frac{\partial u_i}{\partial Z}$ at node j
$\phi_i \Big\vert_k$	$\frac{\partial v_i}{\partial Z}$ at node k
$\lfloor\ \rfloor$	Row vector
$\{\ \}$	Column vector
$[\ ]$	Square matrix
$\mathbf{B}$	Global boundary node force vector
$[C]$	Global damping matrix
$[C_A]^{(e)}$	Elemental damping matrix due to axial internal flow
$[C_{CR}]^{(e)}$	Elemental damping matrix due to cross flow
$[C_T]^{(e)}$	Elemental damping matrix of tube
$[D]$	Dynamic matrix
$\{f\}$	Global external force vector
$[I]$	Unit matrix
$[K]$	Global stiffness matrix
$[K_A]^{(e)}$	Elemental stiffness matrix due to axial internal flow
$[K_{CR}]^{(e)}$	Elemental stiffness matrix due to cross flow
$[K_T]^{(e)}$	Elemental stiffness matrix of tube

$[M]$	Global mass matrix
$[M_A]^{(e)}$	Elemental mass matrix due axial internal flow
$[M_{CR}]^{(e)}$	Elemental mass matrix due to cross flow
$[M_T]^{(e)}$	Elemental mass matrix of tube
$[N]$	Row vector containing shape functions
$[N']$	First derivate of shape functions with respect to Z
$[N'']$	Second derivate of shape functions with respect to Z
$\{u_i\}^{(ne)}$	Nodal X direction diplacement vector of the finite element.
$\{u_i\}^{(ne)}$	Nodal X direction velocity vector of the finite element.
$\{u_i\}^{(ne)}$	Nodal X direction acceleration vector of the finite element.
$\{v_i\}^{(ne)}$	Nodal Y direction displacement vector of the finite element.
$\{v_i\}^{(ne)}$	Nodal Y direction velocity vector of the finite element.
$\{v_i\}^{(ne)}$	Nodal Y direction acceleration vector of the finite element.

SYNOPSIS

Flow Induced Vibration is a major problem in pipelines, heat-exchangers and nuclear reactor cores. Reducing the level of th: vibration has great technical importance in general, whereas in the nuclear reactor it gains its importance from the safety point of view also. To understand the basic mechanism behind this phenomenon considerable research work has been done in the past two decades. Still, some of the mechanisms are remaining fuzzy, especially that in the cross flow induced vibrations.

Recently a mathematical model has been proposed for analysing cross flow induced vibrations in tube banks, using 2-dimensional potential flow fluid forces. In the present work, this model is extended to the combined cross and axial internal flow. Using this model, the Finite Element solution for vibration of a tube bank in stationary outside fluid, as its special case, is obtained and it is comparable with the available earlier results. Results have also been obtained by FEM, for tube banks in (a) stationary fluid, (b) cross flow and (c) combined cross and axial internal flow, using the fluid forces obtained from potential flow theory and experiments, for a class of parameters such as outside fluid mass ratio, gap to radius ratio, number of tubes and axial flow velocity. In (b) and (c) cases, the potential flow theory predicts buckling mode of instability whereas the experimental results predicted dynamic instability. Use of experimentally measured coefficients also predicts the dynamic instability. So to establish close correlation with the experimenta results, the analytical formulation for finding the fluid forces

CHAPTER-I

INTRODUCTION

1.1 INTRODUCTION TO FLOW-INDUCED VIBRATIONS :

The flow of fluid through and around the cylindrical structures, can cause destructive vibrations. These vibrations are induced by the fluid-structure interaction, i.e. the forces exerted by the fluid cause the structure to deform ; as the structure deforms, it changes its orientation to the flow and the fluid forces may change. This dynamic interaction may tend to increase in the vibration of the structure and can cause instability.

Based on the configration of flow, the problems associated with this phenomenon of vibration can be classified as having been induced by

(i) internal axial flow,

(ii) external axial flow,

(iii) cross flow and

(iv) annular flow

In case of axial internal flow, the fluid flowing through the pipe induces the vibrations. Failures due to this vibration are reported in oil pipelines, heat-exchanger tubes and pump discharge lines [1,2]. The mechanism of this flow induced vibration is well understood but the means of prediction of the excitation field are not yet adequate.

In case of external axial flow, the fluid, which induces the vibrations, is flowing outside the tubes and it is parallel to axis of the tubes. This type of flow occurs in heat-exchangers (parallel and counter flow) and nuclear reactor fuel bundles. The vibration characteristics of the external axial flow are in many ways similar to the axial internal flow. Here also the mechanism of this flow-induced problem is well understood but the prediction techniques need further improvements.

A large number of cross flow-induced vibrations are reported in transmission lines, tall chimney structures, closely packed tubes in heat-exchangers and nuclear reactor core [1,2]. In these cases, the fluid flowing across the structures induces the vibration. Several excitation mechanism are possible in cross flow and they are

1. vortex shedding,
2. fluid-elastic instability,
3. turbulent buffeting and
4. acoustic resonance.

Except fluid-elastic instability, all other mechanism are possible in cross flow induced vibration of a single cylindrical structure. In this case, the mechanism of the vortex shedding with or without acoustic resonance is well understood but the turbulent buffeting mechanism needs further investigation. The available prediction methods are inadequate.

In case of cross flow-induced vibration in tube banks, several type of excitation mechanisms can occur simultaneously and it is difficult to identify which is dominating at what place. In fluid-elastic mechanism, the tubes whirl in an oval orbit at flow velocity above a critical velocity. The phenomenon behind this fluid-elastic instability is not fully understood. Even though some methods of prediction are available for this mechanism, they are inadequate. From the failures reported under cross flow-induced vibration, [1], it is noted that most of the failures are caused by fluid-elastic instability.

Some annular flow induced vibrations are reported in some major components of the nuclear reactor, e.g. the thermal shield and core barrel which lie concentrically within the pressure vessel, separated from one another by liquid annules [1 A considerable amount of work has been done on the dynamics of cylinders containing or being immersed in annular flow. The fundamental mechanism for this vibration is fairly well understood but the complexity of geometry and flow fields make vibration prediction sometime difficult.

In the present work, the effects of (a) cross flow (b) combined cross and axial internal flow induced vibration in tube banks have been studied. So, the previous research works which are related to this field are reviewed in the next section.

1.2 REVIEW OF PREVIOUS WORKS :

A comprehensive review about the research works done in axial flow-induced vibration are available in [2,3,4]. In early 1950, the vibration of a fluid conveying pipe was studied in conjuction with the axial flow-induced vibration of the trans-Arabian pipeline. The equation of motion of a fluid conveying pipe was derived by Housner [5]and he solved this equation for the trans-Arabian pipeline geometry . For the simply-supported pipe, he found that at low axial flow velocity, there was negligible effect upon the vibration of pipeline but at a certain high velocity, the pipe buckled like a column subjected to axial loading. Gregory and Paidussis [6]studied the axial flow-induced vibration in cantilever pipes and they showed that at sufficient high axial flow velocity, the cantilever pipes failed due to flutter type of instability. The effect of internal pressure of the fluid was studied theoretical and experimentally by Naguleswaran and Williams [7]. In this case, they found that the effect was similar to the axial flow velocity, i.e. the pipe can become unstable at low-axial flow velocity by the action of internal pressure. Chen [8] studied the effect of displacement and rotational springs at the free end of the cantilever pipe. Using finite element method, Deb and Kumar [9,10]analysed this problem and studied the effect of different kinds of boundary conditions including

multiple supports on the stability of the pipes conveying fluid.

The dynamics and stability of a pipe conveying fluid with pulsating components of axial flow velocity was studied by Paidoussis and Issid [3] . Mishra [11] studied the inplane and outof plane vibration of curved and U-pipelines, using finite element method. Recently in 1986, To and Kaladi [12] adopted the transfer matrix method for the study of vibration of pipelines.

A brief review about cross flow-induced vibration is available in [1,13,14] . In this, the vortex shedding mechanism has attracted the attention of investigators for many years. The vortex shedding behind a stationary cylinder can be described by the Strouhal number, $S=2f_s R/U_o$ (R= cylinder radius, U_o= cross flow velocity and f_s = vortex shedding frequency). In case of a single cylinder, this number is equal to 0.2 and 0.3 for $Re \leq 2x10^5$ and $Re \geq 3.5 \times 10^6$ respectively [1]. (Re= Reynolds number). In other ranges of Re , S is not sharply defined. An important phenomenon associated with vortex shedding excitation is lock-in. i.e., the vortex shedding frequency may concide with the natural frequency of the cylinder. In this lock-in region, the vortex shedding mechanism causes the instability.

Earlier researchers had doubts about the existence of vortex shedding in closely packed tube banks, because of

insufficient space for the shear layers to roll up in classical manner. But later investigations proved that the vortex shedding was possible in atleast first few rows [15] and Strouhal numbers associated with flow across different layout of tube banks are available [2]. Pettigrew and Sylvestre [15] studied this vortex shedding excitation in liquid cross flow tube arrays. This phenomenon appears to be absent in two phase flow and it remains fuzzy . There is a possibility of the concidence of vortex shedding frequency with acoustic of the flow channel and the natural frequency of the tube banks. Such a case may lead to the damage of the heat-exchangers [1].

Connors [16] was the first investigator to recognize the fluid-elastic mechanism of vibrations caused in the tube banks subjected to cross flow. Based on the experimental mode shape, he measured the quasi-steady fluid-elastic forces and developed a simple stability criteria for a tube-row subjected to cross flow in terms of reduced cross flow velocity, $U_r = \frac{U_o}{2fR}$, and mass-damping parameter, $\delta_m = \frac{\pi \tau m}{2\rho R^2}$, (f= natural frequency of the tube, τ = damping ratio, m= mass per unit length of the tube and ρ = density of the cross flow fluid).

$$U_r = k\, \delta_m^{0.5} \qquad (1.1)$$

where k is a dimensionless instability constant and is a function of fluid forces which in turn depend on array geometry.

He obtained the quasi-steady fluid forces by assuming that the dynamic fluid forces acting on a tube at any instant were given by steady fluid forces acting on that particular instantaneous position and its neighbouring tubes. Connors [16] found that k = 9.9 for his tube-row and Eqn. (1.1) has been extensively used as a design guideline for the prevention of fluid-elastic instability of heat-exchanger tube array.

Belvins [17] extended the model to include the variable tube-to-tube stiffness and damping. He also attempted to find an expression for the stability constant of a full tube array, using theoretically determined fluid forces [18]. In his book [2], he suggested that the additional flow velocity-dependent damping terms should be included in the equation of motion of the tubes.

In the above models, the stability curve was found by assumed mode shape of vibration of the tubes. Price and Paidoussis [19] have relaxed the assumption of mode shape, instead the measured fluid force coefficients are inserted into the equations of motion of two-row array and stability is examined using an eigen value analysis. In this way, the least stable mode of vibration is predicted, it being the eigen vector corresponding to eigen values of the lowest critical cross flow velocity.

The mathematical approach used by [16,18,19] includes multiple tubes with fluid-elastic and fluid-damping couplings but the fluid-inertia coupling, which is important for closely packed tube banks vibrating in dense fluid, is not accounted. Chen [20-22] studied the fluid-inertia coupling effects on vibration of group of circular cylinders in (a) unbounded and (b) bounded ideal still fluid. Using 2-dimensional potential flow theory, he found the fluid-inertia coupling between the tubes. He extended the potential flow theory to the cross flow problem, [23], for finding out the fluid-inertia, fluid-damping and fluid-elastic coefficients. These coefficients are dependent upon the array geometry and are independent of cross flow velocity.

Tanaka and Takahara [24] were able to experimentally determine these fluid force coefficients for water flow across a row of tubes and a square array and found them to be dependent on the cross flow velocity as well as the motion of the tube in question and its nearest neighbours. They were able to perform a numerical stability analysis to determine the least stable mode of vibration and generated a stability curve covering the region of their water test. Chen [25] used the Tanaka-Takahara force coefficients and extended the stability curve into the air-flow region. Some interesting jumps or discontinuities in the stability curves were observed by both group of researchers.

Number of conferences have been held in the flow induced vibrations area and the papers presented in some of the conferences are available in [28-31].

1.3 OBJECTIVES AND SCOPE OF PRESENT WORK :

The present work describes the finite element analysis of tube banks vibrating in (a) stationary outside fluid, (b) cross flow and (c) combined cross and axial internal flow. The finite element formulation of the flow induced vibration uses the standard Galerkin finite element method.

The finite element method is tested with the vibration of simply-supported tube-row in a stationary fluid, using 2-dimensional potential flow fluid forces. The finite element solution is compared with that of the closed form solution of Chen [20]. Also the effect of parameters (a) outside fluid mass ratio, ν, (b) gap to radius ratio, G/R, and (c) the number of tubes, K on the natural frequencies of the tube banks are studied. In addition to this, different type of single span and multispan tube-rows are analysed.

In the case of cross flow, the critical cross flow velocity at which the stability occurs first is studied for different layout of tube banks. The fluid forces acting on the tubes due to cross flow are obtained from 2-dimensional potential flow theory. Experimentally measured fluid forces are also used for analysing tube-row. The stability of the system is determined

by the eigen values of the system. Lastly the combined cross and axial internal flow is studied for a row of 5 tubes. The potential flow and experimentally measured fluid forces are used for the stability analysis.

In Chapter II, the equations of motion for the combined cross and axial internal flow are derived and its finite element formulation is given. Formulation for cases cited above, i.e., (a) stationary outside fluid and (b) cross flow are special cases of this formulation.

Chapter-III presents results for all the three cases mentioned above. For the stationary outside fluid, parameters considered are outside fluid mass ratio, gap to radius ratio and the number of tubes in a row. For the cross flow, effect of mass-damping parameter on the critical cross flow velocity has been studied. Whereas for the combined cross and axial internal flow, the critical cross flow velocity has been found out for different mass-damping parameter and axial internal flow velocity. Based on the results and discussion, conclusions are derived and are stated in Chapter IV.

CHAPTER II

EQUATION OF MOTION AND FEM FORMULATION

In this chapter, the equations of motion for a bundle of circular tubes subjected to the combined cross flow and axial internal flow are derived. To obtain the solution of these simultaneous partial differential equations for various boundary conditions and multiple supported tubes, Galerkin finite element method is used to convert these into simultaneous ordinary differential equations.

2.1 EQUATIONS OF MOTION :

A bundle of K tubes subjected to cross flow is shown in Fig.1. The axes of the tubes are parallel to Z- axis and the cross flow is parallel to the X-axis with velocity U_o. The subscript i is used to denote variables associated with tube i, Thus E_i I_i and m_i are the flexural rigidity and mass per unit length of the tube i.

The equation of motion for tube i in the X direction is

$$E_i I_i \frac{\partial^4 u_i}{\partial Z^4} + c_i \frac{\partial u_i}{\partial t} + m_i \frac{\partial^2 u_i}{\partial t^2} = f_i \quad , \; i = 1,2,3,\ldots,K \qquad (2.1)$$

where u_i, c_i and f_i are displacement, structural damping coefficient and fluid forces per unit length in X direction. Similarly, the equation of motion in Y direction is

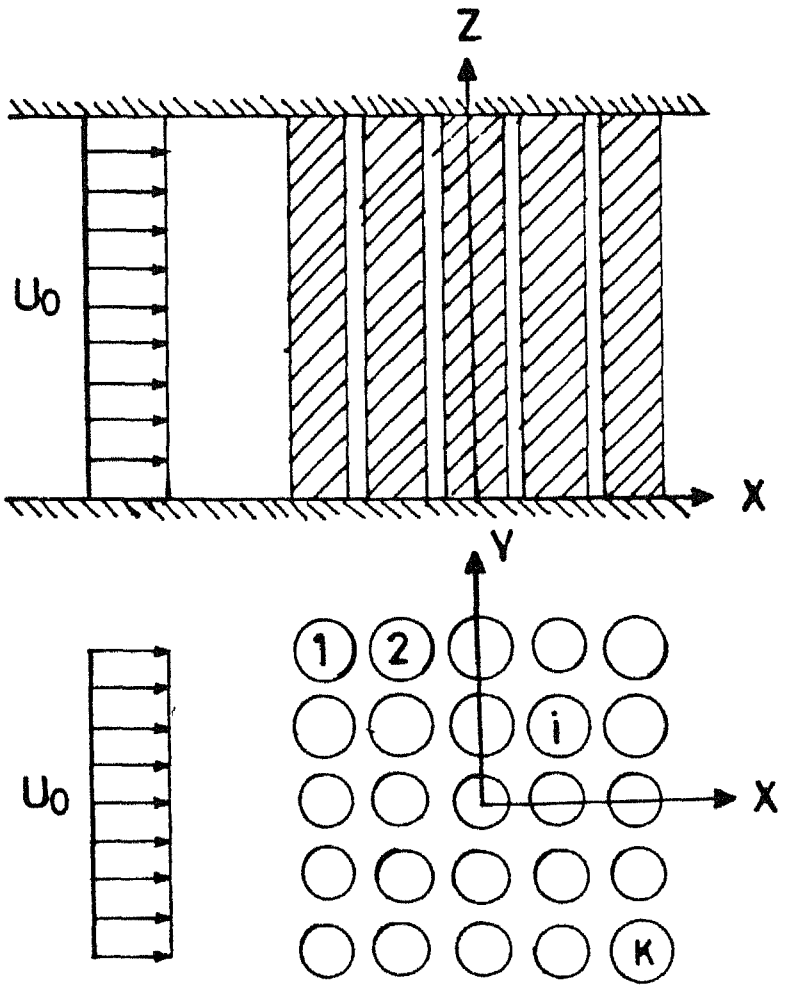

Fig.1 Bundle of Tubes in Cross Flow.

$$E_i I_i \frac{\partial^4 v_i}{\partial z^4} + e_i \frac{\partial v_i}{\partial t} + m_i \frac{\partial^2 v_i}{\partial t^2} = g_i \ , \quad i=1,2,3,\ldots,K \qquad (2.2)$$

where v_i, e_i and g_i are displacement, structural damping coefficient and fluid forces per unit length in Y direction.

With the following assumptions :

1. The fluid flowing across the tube bank is inviscous, incompressible and unbounded.
2. The cross flow is irrotational one.
3. The amplitude of tube motion below the stability threshold is very small.
4. There is no separation of flow.

the fluid forces f_i and g_i are calculated for tube banks arranged in arbitrary pattern, using two dimensional potential flow theory, Chen[23, 25] . In this approach the fluid velocity potential is expressed as a truncated series of unknown coefficients. The boundary conditions are imposed by transforming, the velocity potential to the tubes natural coordinates. The unknown coefficients are computed by solving set of equations which are obtained by imposing boundary conditions. The fluid forces are calculated from fluid pressure acting on the tubes and are.

$$f_i = -\rho\pi \sum_{j=1}^{K} \left(\frac{R_i+R_j}{2}\right)^2 \left(\alpha_{ij} \frac{\partial^2 u_j}{\partial t^2} + \sigma_{ij} \frac{\partial^2 v_j}{\partial t^2}\right) - \rho R_i U_o \sum_{j=1}^{K} \left(\alpha'_{ij} \frac{\partial u_j}{\partial t} + \sigma'_{ij} \frac{\partial v_j}{\partial t}\right)$$

$$+ \rho U_o^2 \sum_{j=1}^{K} \left(\alpha''_{ij} u_j + \sigma''_{ij} v_j\right) + \rho R_i U_o^2 \alpha_i$$

$$g_i = -\rho\pi \sum_{j=1}^{K} \left(\frac{R_i+R_j}{2}\right)^2 \left(\tau_{ij} \frac{\partial^2 u_j}{\partial t^2} + \beta_{ij} \frac{\partial^2 v_j}{\partial t^2}\right) - \rho R_i U_o \sum_{j=1}^{K} \left(\tau'_{ij} \frac{\partial u_j}{\partial t} + \beta'_{ij} \frac{\partial v_j}{\partial t}\right)$$

$$+ \rho U_o^2 \sum_{j=1}^{K} \left(\tau''_{ij}\, u_j + \beta''_{ij}\, v_j\right) + \rho R_i\, U_o^2\, \beta_i \qquad (2.3)$$

where

α_{ij}, σ_{ij}, τ_{ij}, β_{ij} - added mass coefficients,

α'_{ij}, σ'_{ij}, τ'_{ij}, β'_{ij} - fluid damping coefficients,

α''_{ij}, σ''_{ij}, τ''_{ij}, β''_{ij} - fluid-elastic stiffness coefficients,

α_i - X component of steady state fluid force coefficients,

β_i - Y component of steady state fluid force coefficients,

ρ - density of cross flow fluid,

U_o - cross flow fluid velocity,

R - outside radius of tube.

The equations of motion for flexural vibration of a uniform tube i subjected to axial internal flow V_{ai} are, [3],

$$E_i I_i \frac{\partial^4 u_i}{\partial Z^4} + (m_i+m_{ai}) \frac{\partial^2 u_i}{\partial t^2} + 2m_{ai} V_{ai} \frac{\partial^2 u_i}{\partial Z \partial t} + m_{ai} V_{ai}^2 \frac{\partial^2 u_i}{\partial Z^2} = 0$$

$$E_i I_i \frac{\partial^4 v_i}{\partial Z^4} + (m_i+m_{ai}) \frac{\partial^2 v_i}{\partial t^2} + 2m_{ai} V_{ai} \frac{\partial^2 v_i}{\partial Z\, \partial t} + m_{ai} V_{ai}^2 \frac{\partial^2 v_i}{\partial Z^2} = 0 \qquad (2.4)$$

where

m_{ai} - mass per unit length of internal fluid.

From Eqns.(2.1) to (2.4), one can get the equations of motion for a bundle of tubes subjected to the combined cross flow U_o, and axial internal flow V_{ai}, as follows

$$E_iI_i \frac{\partial^4 u_i}{\partial Z^4} + m_{ai}V_{ai}^2 \frac{\partial^2 u_i}{\partial Z^2} - \rho U_o^2 \sum_{j=1}^{K} (\alpha''_{ij} u_j + \sigma''_{ij} v_j) + c_i \frac{\partial u_i}{\partial t}$$
$$+2m_{ai}V_{ai} \frac{\partial^2 u_i}{\partial Z\, \partial t} + \rho R_i U_o \sum_{j=1}^{K} (\alpha'_{ij} \frac{\partial u_j}{\partial t} + \sigma'_{ij} \frac{\partial v_j}{\partial t}) + (m_i + m_{ai}) \frac{\partial^2 u_i}{\partial t^2}$$
$$+\pi\rho \sum_{j=1}^{K} \left(\frac{R_i+R_j}{2}\right)^2 (\alpha_{ij} \frac{\partial^2 u_j}{\partial t^2} + \sigma_{ij} \frac{\partial^2 v_j}{\partial t^2}) - \rho R_i U_o^2 \alpha_i = 0 \qquad (2.5a)$$

$$E_iI_i \frac{\partial^4 v_i}{\partial Z^4} + m_{ai}V_{ai}^2 \frac{\partial^2 v_i}{\partial Z^2} - \rho U_o^2 \sum_{j=1}^{K} (\tau''_{ij} u_j + \beta''_{ij} v_j) + e_i \frac{\partial v_i}{\partial t}$$
$$+2m_{ai}V_{ai} \frac{\partial^2 v_i}{\partial Z^2} + \rho R_i U_o \sum_{j=1}^{K} (\tau'_{ij} \frac{\partial u_j}{\partial t} + \beta'_{ij} \frac{\partial v_j}{\partial t}) + (m_i + m_{ai}) \frac{\partial^2 v_i}{\partial t^2}$$
$$+\pi\rho \sum_{j=1}^{K} \left(\frac{R_i+R_j}{2}\right)^2 (\tau_{ij} \frac{\partial^2 u_j}{\partial t^2} + \beta_{ij} \frac{\partial^2 v_j}{\partial t^2}) - \rho R_i U_o^2 \beta_i = 0 \qquad (2.5b)$$

$$i = 1,2,3,\ldots,K$$

In the present work, all tubes have been taken as uniform and identical. Thus length, radius, mass, flexural rigidity and structural damping coefficients of all tubes are equal. Also fluid flowing through and its velocity are same for all tubes. So

$$R_i = R \; ; \; m_i = m \; ; \; m_{ai} = m_a$$
$$V_{ai} = V_a ; \; E_iI_i = EI ; \; c_i = e_i = c \qquad (2.6)$$

2.2 FEM FORMULATION :

All tubes are divided into (q-1) elements with q nodes, see Fig. 2. Typical finite element is also shown in the same figure. The displacements $u_i^{(e)}$ and $v_i^{(e)}$ over the typical element of a representative tube i are taken as

$$u_i^{(e)}(Z,t) = \sum_{r=1}^{a} N_r(Z)\, u_i(t) = \lfloor N \rfloor \{u_i(t)\}^{(ne)}$$
$$v_i^{(e)}(Z,t) = \sum_{r=1}^{b} M_r(Z)\, v_i(t) = \lfloor M \rfloor \{v_i(t)\}^{(ne)} \qquad (2.7)$$

where

a - number of degrees of freedom associated with u displacemen

b - number of degrees of freedom associated with v displacemen

$\lfloor N \rfloor$ - shape function for u displacement

$\lfloor M \rfloor$ - shape function for v displacement

Substituting Eqns. (2.7) in Eqns. (2.5) residues Ru_i and Rv_i are obtained. These residues are minimized by the Galerkin method, thus

$$\int_0^h N_r\, Ru_i\, dZ = 0$$
$$\int_0^h M_r\, Rv_i\, dZ = 0 \qquad (2.8)$$
$$i = 1,2,\ldots,K.$$

Eqns. (2.8) are integrated by parts as much as possible. It is seen that the highest order of derivatives of u and v are two in the integrals and three in the whole equations.

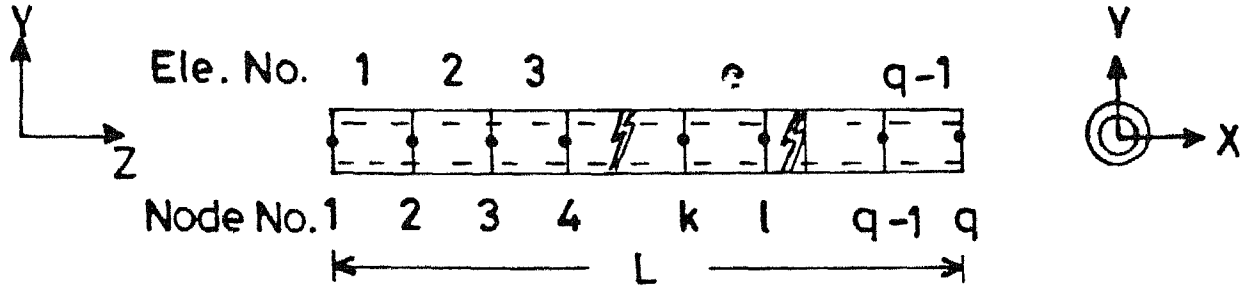

Nodes and Finite Elements of Tube i

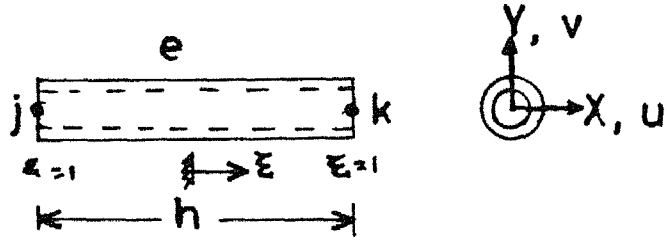

Typical Finite Element

Fig. 2 Finite Element Representation.

To ensure monotonic convergence, the C_1 element should be used for both u and v . The shape function for this elements are given as,

$$\lfloor N \rfloor = \lfloor M \rfloor = \lfloor \frac{1}{4}(2-3\xi+\xi^3) \quad \frac{h}{8}(1-\xi-\xi^2+\xi^3) \quad \frac{1}{4}(2+3\xi-\xi^3) \quad \frac{h}{8}(-1-\xi+\xi^2+\xi^3) \rfloor \qquad (2.9)$$

where $\xi = \dfrac{Z^{(e)} - (Z_k + Z_j)/2}{(Z_k - Z_j)/2}$; $h = Z_k - Z_j$

Using these shape functions, Eqns. (2.8) which have been integrated by parts can be written in matrix form as

$$EI \int_o^h \{N''\}\lfloor N''\rfloor dZ \{u_i\}^{(ne)} - m_a V_a^2 \int_o^h \{N'\}\lfloor N'\rfloor dZ \{u_i\}^{(ne)}$$

$$-\rho U_o^2 \sum_{j=1}^{K} \left(\alpha''_{ij} \int_o^h \{N\}\lfloor N\rfloor dZ \{u_j\}^{(ne)} + \sigma''_{ij} \int_o^h \{N\}\lfloor N\rfloor dZ \{v_j\}^{(ne)} \right)$$

$$+c \int_o^h \{N\}\lfloor N\rfloor dZ \{\dot{u}_i\}^{(ne)} + 2m_a V_a \int_o^h \{N\}\lfloor N'\rfloor dZ \{\dot{u}_i\}^{(ne)}$$

$$+\rho R U_o \sum_{j=1}^{K} \left(\alpha'_{ij} \int_o^h \{N\}\lfloor N\rfloor dZ \{\dot{u}_j\}^{(ne)} + \sigma'_{ij} \int_o^h \{N\}\lfloor N\rfloor dZ \{\dot{v}_j\}^{(ne)} \right)$$

$$+(m+m_a) \int_o^h \{N\}\lfloor N\rfloor dZ \{\ddot{u}_i\}^{(ne)} + \pi\rho R^2 \sum_{j=1}^{K} \left(\alpha_{ij} \int_o^h \{N\}\lfloor N\rfloor dZ \{\ddot{u}_j\}^{(ne)} \right.$$

$$\left. + \sigma_{ij} \int_o^h \{N\}\lfloor N\rfloor dZ \{\ddot{v}_j\}^{(ne)} \right) - \rho R U_o^2 \alpha_i \int_o^h \{N\} dZ$$

$$+ \{N\} EI \frac{\partial^3 u_i^{(e)}}{\partial Z^3} \Big|_o^h - \{N'\} EI \frac{\partial^2 u_i}{\partial Z^2} \Big|_o^h + \{N\} m_a V_a^2 \frac{\partial u_i^{(e)}}{\partial Z} \Big|_o^h = \{0\}$$

(2.10a)

$$EI \int_0^h \{N''\}[N'']\,dZ\{v_i\}^{(ne)} - m_a V_a^2 \int_0^h \{N'\}[N']\,dZ\{v_i\}^{(ne)}$$

$$- \rho U_o^2 \sum_{j=1}^{K} \left(\tau''_{ij} \int_0^h \{N\}[N]dZ\{u_j\}^{(ne)} + \beta''_{ij} \int_0^h \{N\}[N]dZ\{v_j\}^{(ne)}\right)$$

$$+c \int_0^h \{N\}[N]\,dZ\{\dot{v}_i\}^{(ne)} + 2m_a V_a \int_0^h \{N\}[N']\,dZ\{\dot{v}_i\}^{(ne)}$$

$$+\rho R U_o \sum_{j=1}^{K} \left(\tau'_{ij} \int_0^h \{N\}[N]\,dZ\{\dot{u}_j\}^{(ne)} + \beta'_{ij} \int_0^h \{N\}[N]dZ\{\dot{v}_j\}^{(ne)}\right)$$

$$+(m+m_a) \int_0^h \{N\}[N]\,dZ\{\ddot{v}_i\}^{(ne)} + \pi\rho R^2 \sum_{j=1}^{K} \left(\tau_{ij} \int_0^h \{N\}[N]\,dZ\{\ddot{u}_j\}^{(ne)}\right.$$

$$\left.+\beta_{ij} \int_0^h \{N\}[N]\,dZ\{\ddot{v}_j\}^{(ne)}\right) - \rho R U_o^2 \beta_i \int_0^h \{N\}\,dZ$$

$$+\{N\} EI \frac{\partial^3 v_i^{(e)}}{\partial Z^3}\Big|_0^h - \{N'\} EI \frac{\partial^2 v_i^{(e)}}{\partial Z^2}\Big|_0^h + \{N\} m_a V_a^2 \frac{\partial v_i^{(e)}}{\partial Z}\Big|_0^h = \{0\}$$

(2.10b)

Eqn. (2.10) can be written as

$$\sum_{j=1}^{K} \left((\delta_{ij}[K_T]^{(e)} - \delta_{ij}[K_A]^{(e)} - \alpha''_{ij}[K_{CR}]^{(e)})\{u_j\}^{(ne)}\right.$$

$$-\sigma''_{ij}[K_{CR}]^{(e)}\{v_j\}^{(ne)} + (\delta_{ij}[C_T]^{(e)} + \delta_{ij}[C_A]^{(e)} + \alpha'_{ij}[C_{CR}]^{(e)})\{\dot{u}_j\}^{(ne)}$$

$$+\sigma'_{ij}[C_{CR}]^{(e)}\{\dot{v}_j\}^{(ne)} + (\delta_{ij}[M_T]^{(e)} + \delta_{ij}[M_A]^{(e)} + \alpha_{ij}[M_{CR}]^{(e)})\{\ddot{u}_j\}^{(r}$$

$$\left.+\sigma_{ij}[M_{CR}]^{(e)}\{\ddot{v}_j\}^{(ne)}\right) = \alpha_i \{F_{CR}\}^{(e)} + \{B_u\}_i^{(e)}$$

(2.11a)

$$\sum_{j=1}^{K} (-\tau''_{ij} [K_{CR}]^{(e)} \{u_j\}^{(ne)} + (\delta_{ij}[K_T]^{(e)} - \delta_{ij} [K_A]^{(e)}$$

$$-\beta''_{ij} [K_{CR}]^{(e)}) \{v_j\}^{(ne)} + \tau'_{ij} [C_{CR}]^{(e)} \{\dot{u}_j\}^{(ne)} + (\delta_{ij} [C_T]^{(e)}$$

$$+\delta_{ij} [C_A]^{(e)} + \beta'_{ij} [C_{CR}]^{(e)}) \{\dot{v}_j\}^{(ne)} + \tau_{ij} [M_{CR}]^{(e)} \{\ddot{u}_j\}^{(ne)}$$

$$+ (\delta_{ij} [M_T]^{(e)} + \delta_{ij} [M_A]^{(e)} + \beta_{ij} [M_{CR}]^{(e)}) \{\ddot{v}_j\}^{(ne)}))$$

$$= \beta_i \{F_{CR}\}^{(e)} + \{B_v\}_i^{(e)} \qquad (2.11b)$$

where δ_{ij} = Kronecker's delta

$[K_T]^{(e)} = EI \int_o^h \{N''\}[N'']dZ$, stiffness matrix due to tube bending ;

$[K_A]^{(e)} = m_a V_a^2 \int_o^h \{N'\}[N']dZ$, stiffness matrix due to axial internal flow ;

$[K_{CR}]^{(e)} = \rho U_o^2 \int_o^h \{N\}[N]\,dZ$, stiffness matrix due to cross flow ;

$[C_T]^{(e)} = c \int_o^h \{N\}[N]\,dZ$, damping matrix of tube ;

$[C_A]^{(e)} = 2m_a V_a \int_o^h \{N\}[N']\,dZ$, damping matrix due to axial internal flow ;

$[C_{CR}]^{(e)} = \rho R U_o \int_o^h \{N\}[N]\,dZ$, damping matrix due to cross flow ;

$[M_T]^{(e)} = m \int_o^h \{N\}[N]\,dZ$, mass matrix of the tube ;

$[M_A]^{(e)} = m_a \int_o^h \{N\}[N]\,dZ$, mass matrix due to axial internal flow ;

$[M_{CR}]^{(e)} = \pi \rho R^2 \int_o^h \{N\}[N]\,dZ$, mass matrix due to cross flow ;

$$\{F_{CR}\}^{(e)} = \rho R U_o^2 \int_o^h \{N\} dZ, \text{ force matrix due to cross flow ;}$$

$$\{B_u\}_i^{(e)} = \begin{Bmatrix} EI\dfrac{\partial^3 u_i}{\partial Z^3} + m_a V_a^2\, \theta_i \Big|_j \\ -EI\dfrac{\partial^2 u_i}{\partial Z^2}\Big|_j \\ -EI\dfrac{\partial^3 u_i}{\partial Z^3} - m_a V_a^2\, \theta_i \Big|_k \\ EI\dfrac{\partial^2 u_i}{\partial Z^2}\Big|_k \end{Bmatrix} \text{, X-direction forces at the nodes,}$$

$$\{B_v\}_i^{(e)} = \begin{Bmatrix} EI\dfrac{\partial^3 v_i}{\partial Z^3} + m_a V_a^2\, \phi_i \Big|_j \\ -EI\dfrac{\partial^2 v_i}{\partial Z^2}\Big|_j \\ -EI\dfrac{\partial^3 v_i}{\partial Z^3} - m_a V_a^2\, \phi_i \Big|_k \\ EI\dfrac{\partial^2 v_i}{\partial Z^2}\Big|_k \end{Bmatrix} \text{, Y-direction forces at the nodes.} \qquad (2.12)$$

On assembling, Eqns. (2.11), equations of motion for the i-th tube become

$$\sum_{j=1}^{K} \left([KU1]_{ij}\{u_j\} + [KV1]_{ij}\{v_j\} + [CU1]_{ij}\{\dot{u}_j\} + [CV1]_{ij}\{\dot{v}_j\} \right.$$

$$\left. + [MU1]_{ij}\{\ddot{u}_j\} + [MV1]_{ij}\{\ddot{v}_j\} \right) = \{FU\}_i + \{BU\}_i$$

$$\sum_{j=1}^{K} \left([KU2]_{ij} \{u_j\} + [KV2]_{ij} \{v_j\} + [CV2]_{ij} \{\dot{u}_j\} + [CV2]_{ij} \{\dot{v}_j\} \right.$$

$$\left. + [MV2]_{ij} \{\ddot{u}_j\} + [MV2]_{ij} \{\ddot{v}_j\} \right) = \{FV\}_i + \{BV\}_i \qquad (2.13)$$

where

$$[KU1]_{ij} = \Sigma \left(\delta_{ij} [K_T]^{(e)} - \delta_{ij} [K_A]^{(e)} - \alpha''_{ij} [K_{CR}]^{(e)}\right);$$

$$[KV2]_{ij} = \Sigma \left(\delta_{ij} [K_T]^{(e)} - \delta_{ij} [K_A]^{(e)} - \beta''_{ij} [K_{CR}]^{(e)}\right);$$

$$[KV1]_{ij} = \Sigma - \sigma''_{ij} [K_{CR}]^{(e)}; \quad [KU2]_{ij} = \Sigma - \tau''_{ij} [K_{CR}]^{(e)};$$

$$[CU1]_{ij} = \Sigma \left(\delta_{ij} [C_T]^{(e)} + \delta_{ij} [C_A]^{(e)} + \alpha'_{ij} [C_{CR}]^{(e)}\right);$$

$$[CV2]_{ij} = \Sigma \left(\delta_{ij} [C_T]^{(e)} + \delta_{ij} [C_A]^{(e)} + \beta'_{ij} [C_{CR}]^{(e)}\right);$$

$$[CV1]_{ij} = \Sigma \sigma'_{ij} [C_{CR}]^{(e)}; \quad [CU2]_{ij} = \Sigma \tau'_{ij} [C_{CR}]^{(e)};$$

$$[MU1]_{ij} = \Sigma \left(\delta_{ij} [M_T]^{(e)} + \delta_{ij} [M_A]^{(e)} + \alpha_{ij} [M_{CR}]^{(e)}\right);$$

$$[MV2]_{ij} = \Sigma \left(\delta_{ij} [M_T]^{(e)} + \delta_{ij} [M_A]^{(e)} + \beta_{ij} [M_{CR}]^{(e)}\right);$$

$$[MV1]_{ij} = \Sigma \sigma_{ij} [M_{CR}]^{(e)}; \quad [MU2]_{ij} = \Sigma \tau_{ij} [M_{CR}]^{(e)};$$

$$\{FU\}_i = \Sigma \alpha_i \{F_{CR}\}^{(e)}; \quad \{FV\}_i = \Sigma \beta_i \{F_{CR}\}^{(e)}$$

$$\{BU\}_i = \Sigma \{BU\}_i^{(e)}; \quad \{BV\}_i = \Sigma \{BV\}_i^{(e)} \qquad (2.14)$$

As said above the Eqns. (2.13) are for a typical tube i.

Clubbing for all tubes, one gets

$$\begin{bmatrix} M \end{bmatrix} \begin{Bmatrix} \{\ddot{u}\} \\ \{\ddot{v}\} \end{Bmatrix} + \begin{bmatrix} C \end{bmatrix} \begin{Bmatrix} \{\dot{u}\} \\ \{\dot{v}\} \end{Bmatrix} + \begin{bmatrix} K \end{bmatrix} \begin{Bmatrix} \{u\} \\ \{v\} \end{Bmatrix} = \{F\} + \{B\} \qquad (2.15)$$

where

$$[M] = \begin{bmatrix} [MU1]_{11} & \cdots & [MU1]_{1k} & [MV1]_{1k} & \cdots & [MV1]_{1k} \\ \vdots & & \vdots & \vdots & & \vdots \\ [MU1]_{k1} & \cdots & [MU1]_{kk} & [MV1]_{k1} & \cdots & [MV1]_{kk} \\ [MU2]_{11} & \cdots & [MU2]_{1k} & [MV2]_{11} & \cdots & [MV2]_{1k} \\ \vdots & & \vdots & \vdots & & \vdots \\ [MU2]_{k1} & & [MU2]_{kk} & [MV2]_{k1} & \cdots & [MV2]_{kk} \end{bmatrix} \qquad (2.16)$$

In the same way $[C]$ and $[K]$ matrices are clubbed

and

$$\{F\} = \begin{Bmatrix} \{FU\}_1 \\ \vdots \\ \{FU\}_k \\ \{FV\}_1 \\ \vdots \\ \{FV\}_k \end{Bmatrix} ; \{B\} = \begin{Bmatrix} \{BU\}_1 \\ \vdots \\ \{BU\}_k \\ \{BV\}_1 \\ \vdots \\ \{BV\}_k \end{Bmatrix} \qquad (2.17)$$

Eqn. (2.16) consists of simultaneous, second order differential equation which can be solved for various type of boundary conditions.

CHAPTER-III

RESULTS AND DISCUSSIONS

In this chapter, the method of solution for the set of differential equations, which are obtained from equations of motion by FEM, is discussed. Then the results for the following three cases are presented.

(i) Vibration of tube banks in stationary fluid

(ii) Vibration of tube banks in cross flow

(iii) Vibration of tube banks subjected to the combined cross and axial internal flow.

The effect of different parameters on these results are also discussed.

3.1 METHOD OF SOLUTION :

The solution for the simultaneous second order ordinary differential equations, Eqn. (2.15), is obtained as explained in Meirovitch [32] and Duncan and Collar [33]. Using generalised velocity of $\{\dot{u}\}$ and $\{\dot{v}\}$ as auxillary variable, n second order differential equations, Eqn. (2.15), are converted to a set of 2n first order differential equations.

$$[\bar{M}]\{\dot{W}\} + [\bar{K}]\{W\} = \{\bar{F}\} \qquad (3.1)$$

where

$$\{W\} = \begin{Bmatrix} \{\dot{u}\} \\ \{\dot{v}\} \\ \{u\} \\ \{v\} \end{Bmatrix} \quad ; \quad \bar{F} = \begin{Bmatrix} \{0\} \\ \{F\} \end{Bmatrix}$$

$$[\bar{M}] = \begin{bmatrix} [O] & [M] \\ [M] & [C] \end{bmatrix} \quad ; [\bar{K}] = \begin{bmatrix} -[M] & [O] \\ [O] & [K] \end{bmatrix}$$

For damped free vibration, eigen values are obtained by assuming the following solution

$$\{W\} = e^{\lambda t} \{\bar{W}\} \tag{3.2}$$

where λ is an eigen value and $\{\bar{W}\}$ is the corresponding eigen vector. Substituting Eqn.(3.2) in the homogenous form of Eqn. (3.1) leads to

$$\lambda [\bar{M}]\{\bar{W}\} + [\bar{K}]\{\bar{W}\} = \{O\} \tag{3.3}$$

or

$$[D]\{\bar{W}\} = \frac{1}{\lambda} [I]\{\bar{W}\}$$

where

$$[D] = -[\bar{K}]^{-1}[\bar{M}] = \begin{bmatrix} [O] & [I] \\ -[K]^{-1}[M] & -[K]^{-1}[C] \end{bmatrix}$$

The eigen values of the dynamic matrix $[D]$, will in general be a complex number. The real part of the eigen value determines stability of the system and imaginary part gives the natural frequency of vibration. If λ is complex, having negative real part, the system is stable and performs damped oscillations. When λ is complex, having positive real part , the system becomes unstable dynamically (flutter). When α is real, then the system loses stability by divergence (buckling).

3.2 DIMENSIONLESS PARAMETERS :

The results are presented in terms of dimensionless parameters used in literature and they are

Inside fluid mass ratio $= \beta = \frac{m_a}{m+m_a}$

Outside fluid mass ratio $= \nu = \frac{\pi \rho R^2}{m+m_a}$

Mass-damping parameter $= \delta_m = \frac{\pi \tau (m+m_a)}{2\rho R^2}$

Dimensionless Axial internal flow velocity $= V = \frac{V_a L}{\sqrt{EI/m_a}}$

Reduced cross flow velocity $= U_r = \frac{U_o}{2f\,R}$

Real part of dimensionless frequency $= Re(\Omega) = \frac{Re(\lambda)}{\sqrt{EI/((m+m_a)L^4)}}$

Imaginary part of dimensionless frequency $= Im(\Omega) = \frac{Im(\lambda)}{\sqrt{EI/((m+m_a)L^4)}}$

where

L - length of tube,

f - fundamental natural frequency of the tube in vacuum (Hz),

τ - damping ratio $\left(\tau = \frac{c}{4\pi\,(m+m_a)f}\right)$

3.3 NUMBER OF FINITE ELEMENTS USED IN EACH TUBE :

In finite element method, the accuracy of the natural frequencies depend upon the number of finite elements used in each tube. To decide the minimum number of elements required for each tube, natural frequencies of a row of 5 simply-supported tubes

are obtained for 1 to 6 number of elements in each tube. The first and second natural frequencies are given in Table 1. It was found that after 4 elements, there was hardly any change in natural frequencies corresponding to first mode of single tube in vacuum. So all results are obtained by taking 4 elements in each tube.

3.4 VIBRATION OF TUBE BANKS IN STATIONARY FLUID :

This case is studied without axial internal flow and damping. Equations of motion are obtained from Eqn. (2.15) by substituting $U_o = m_a = V_a = c = 0$. It is noted that there is a coupling between the tubes in the mass matrix, [M], and it is due to the added mass coefficients. These coefficients are obtainable from the 2-dimensional potential flow theory.

First, the natural frequencies for a number of simply supported tubes (1 to 10) in a row are obtained, gap to radius ratio, G/R, and outside fluid mass ratio, ν , are taken as 0.2 and 0.54267 respectively. These results are shown in Fig. 3 as a function of number of tubes in a row, K. It is known that corresponding to each mode of a single tube in vacuum, there are 2K coupled frequencies for a row of K tubes, [21] . Results in Fig. 3 are first, second, $2K-1^{th}$ and $2K^{th}$ frequencies corresponding to the first mode of single tube in vacuum. The mode shapes for these frequencies are also shown in the same figure. With increase in number of tubes, the first and second frequencies decrease and $2K-1^{th}$ and $2K^{th}$ frequencies increase. All other

Table 1 : NATURAL FREQUENCIES OF A ROW OF 5 SIMPLY SUPPORTED TUBES IN STATIONARY FLUID FOR DIFFERENT NUMBER OF FINITE ELEMENTS IN EACH TUBE ($G/R = 0.2$, $\nu=0.5$, $\tau= 0.0$)

Number of elements in each tube	First Frequency		Second Frequency	
	$Re(\Omega)$	$Im(\Omega)$	$Re(\Omega)$	$Im(\Omega)$
1	0.0	7.0419	0.0	7.7067
2	0.0	6.3696	0.0	6.9708
3	0.0	6.3497	0.0	6.9491
4	0.0	6.3462	0.0	6.9452
5	0.0	6.3452	0.0	6.9442
6	0.0	6.3449	0.0	6.9438

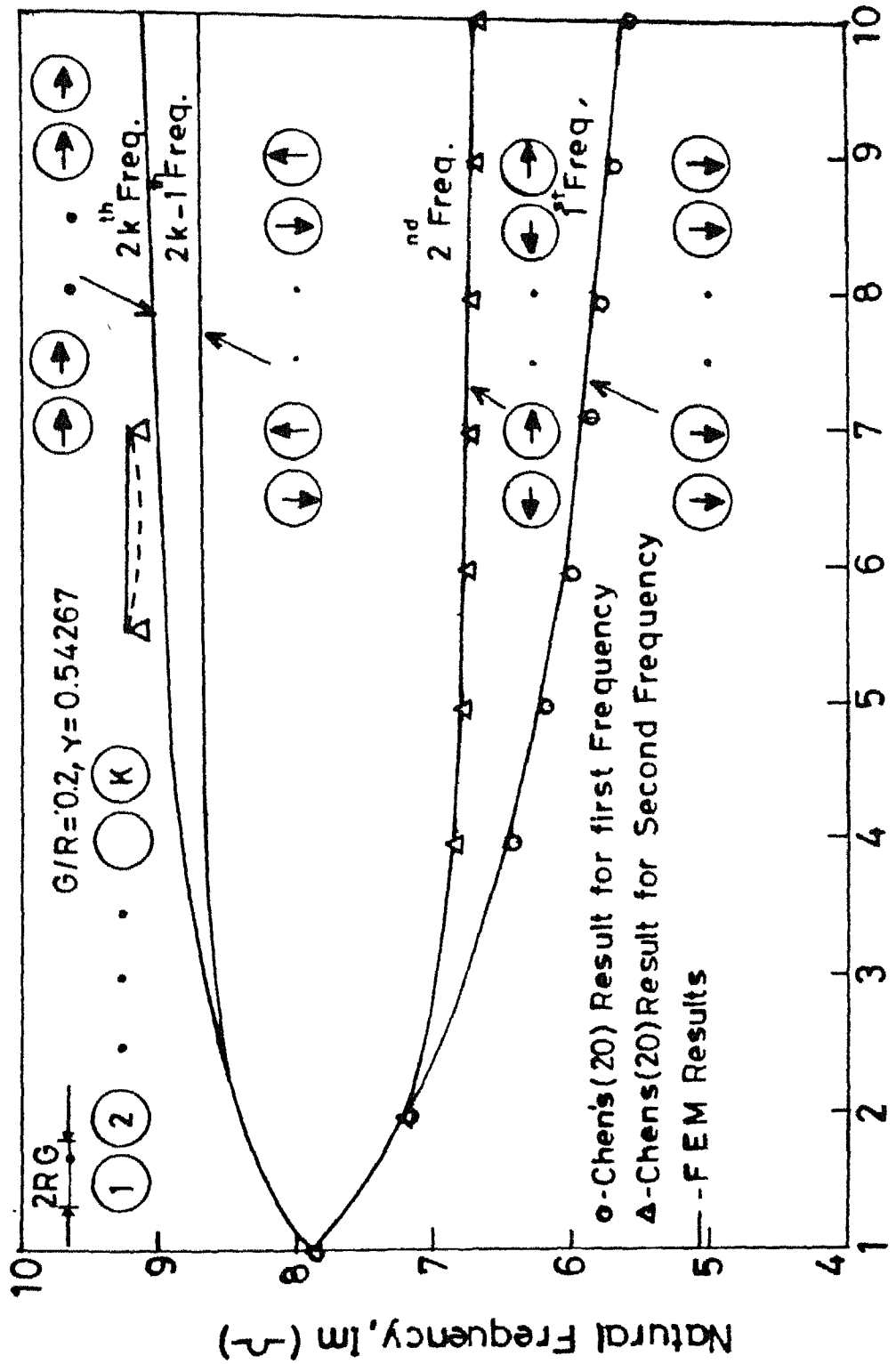

Fig.3 Effect of Number of Tubes on Natural Frequency of a Row of Tubes in Stationary Fluid.

frequencies corresponding to first mode of a single tube lie between the first and $2K^{th}$ frequencies. Results for the first and second frequencies are given by Chen [20] and the present results match well with those results.

Next, the effect of fluid mass ratio, ν, and boundary conditions are studied and the results for the first natural frequency are given in Fig. 4. For mass ratio study, all tubes are taken as simply supported. With increase in mass ratio, ν, all frequencies decrease, as expected. For boundary condition effects, all tubes are taken as fixed-fixed. All frequencies increase considerably as expected. Fig. 4 shows, these effects on the first natural frequency.

Natural frequencies also depend upon the gap to radius ratio, G/R. This effect is studied for a triangular array of 3 simply supported tubes. The arrangements of the tube array and results for the first six frequencies corresponding to first mode of single tube in vacuum are shown in Fig. 5. The gap to radius ratio, G/R, is varied from 0.01 to 1.0. As the G/R ratio increases the first three frequencies increase, the effect being very much pronounced in the first frequency. For the other three frequencies, the trend is opposite. As the spacing increases all the frequencies approach the first mode frequency of a single tube vibrating in infinite fluid, which is shown in dotted line in the Fig. 5. These results also match well with those of Chen [21] . The same trend is also observed in the set of six frequencies corresponding to higher modes of single tube in vacuum, though they are not presented here.

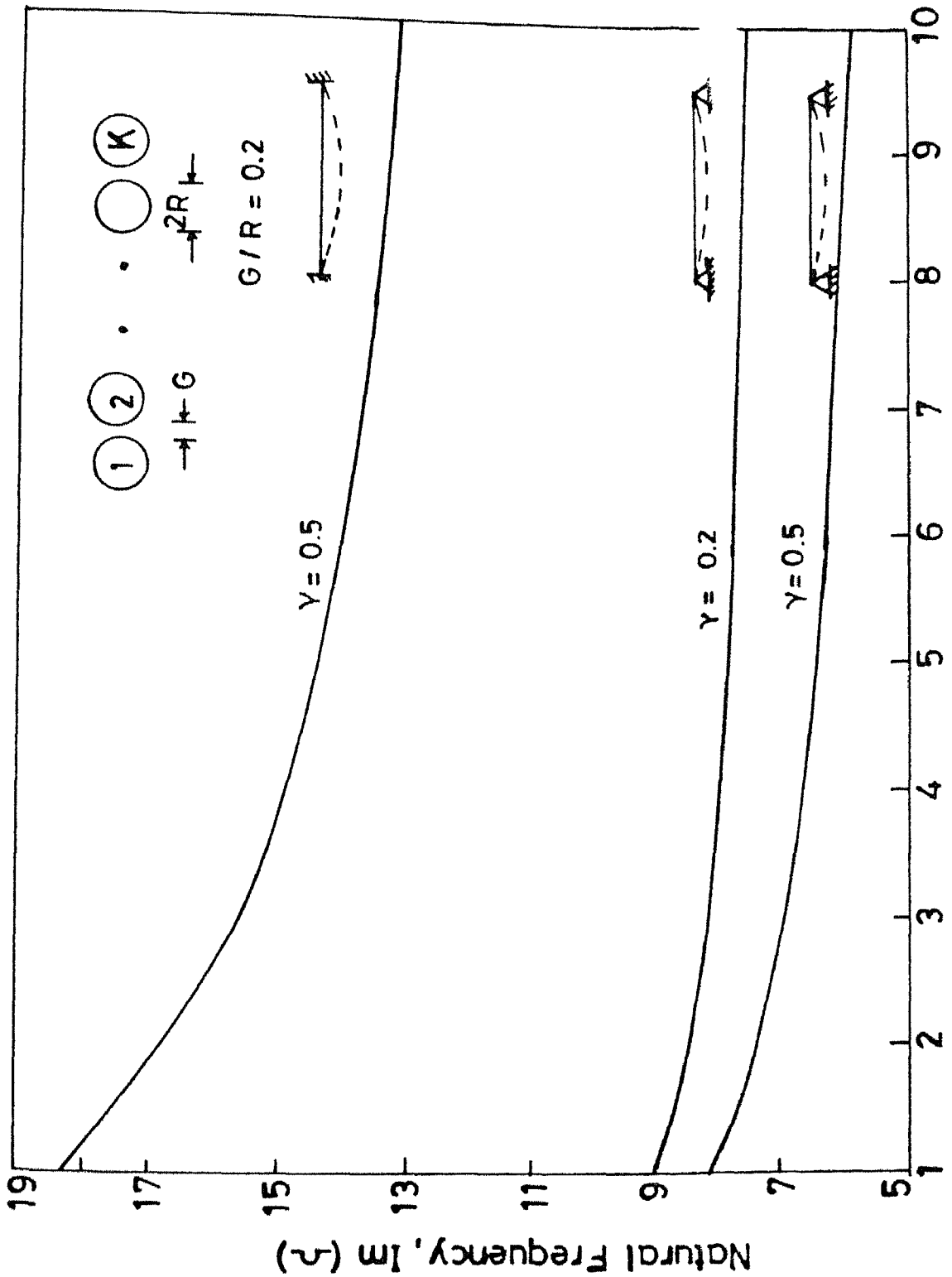

Fig. 4 Effect of Boundary Condition and γ on Funamental Frequency of a Row of Tubes in Stationary Fluid.

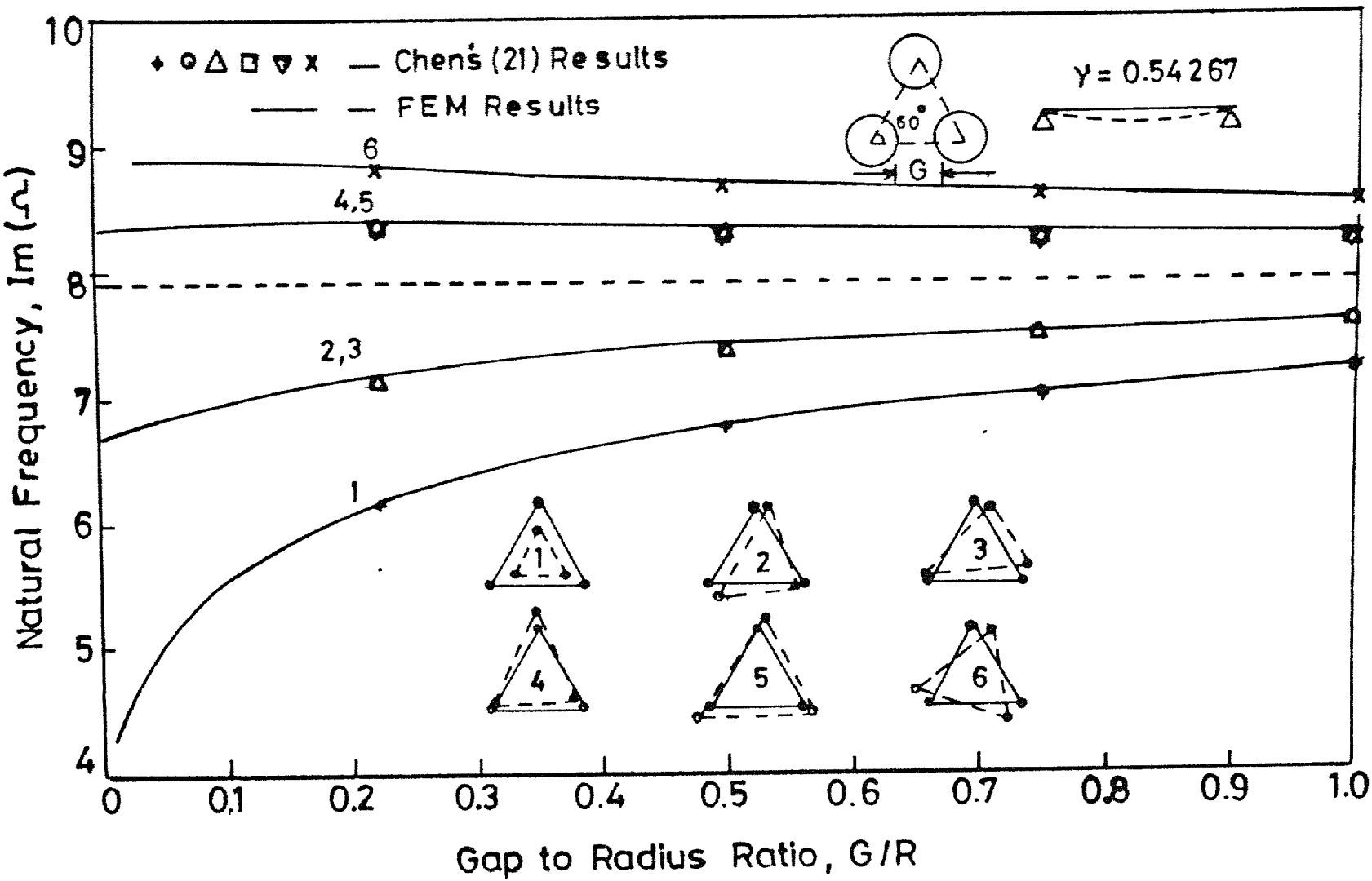

Fig. 5 Effect of Gap to Radius Ratio on Natural Frequencies of a Triangular Array of Tubes in Stationary Fluid.

Lastly the effect of intermediate support on the natural frequencies is studied. The first two natural frequencies of hinged-hinged, fixed-fixed and fixed-hinged tubes, 5 in a row with and without intermediate support are given in Table 2. Introduction of intermediate support in a tube row increases the frequencies, as expected. For these three boundary conditions, the effect is more pronounced in the hinged-hinged tube row.

3.5 VIBRATION OF TUBE BANKS IN CROSS FLOW :

The equations of motion for tube banks vibrating in cross flow can be obtained from Eqn. (2.15) by substituting m_a and V_a as zero. There is a coupling between the tubes in $[M]$, $[C]$ and $[K]$ matrices due to added-mass, fluid-damping and fluid-elastic coefficients. The stability of the tube banks is determined by the eigen values of the system. The instability can be static (buckling) or dynamic (flutter). The cross flow velocity, at which the first instability occurs, is noted as critical cross flow velocity.

In this stability analysis, the damping ratio, τ, and outside fluid mass ratio, ν, can be taken as two independent parameters. But Chen [25] and Blevins [2] found that both parameters appears in the stability criteria as a single parameter, mass-damping parameter, δ_m. They presented the results in terms of this parameter. Same has been followed in this work.

TABLE 2.: NATURAL FREQUENCY OF A ROW OF 5 TUBES IN STATIONARY FLUID FOR DIFFERENT BOUNDARY CONDITIONS, $\nu = 0.5$, $G/R = 0.2$.

BOUNDARY CONDITION	FIRST FREQUENCY		SECOND FREQUENCY	
	Re (Ω)	Im (Ω)	Re (Ω)	Im (Ω)
	0.0	6.346	0.0	6.945
	0.0	25.385	0.0	27.781
	0.0	14.402	0.0	15.761
	0.0	39.671	0.0	43.415
	0.0	9.918	0.0	10.854
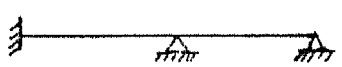	0.0	29.617	0.0	32.413

First, stability of a row of five uniformly spaced, simply-supported tubes is studied. The gap to radius ratio, G/R, and the damping ratio, τ , are taken as 0.66 and 0.02 respectively. The arrangements of the tubes and flow direction are shown in Fig.6. By 2-dimensional potential flow theory, the fluid forces acting on the tubes are calculated and are given in Table 3 to 5. Using these fluid forces, the critical reduced cross flow velocity, U_r^* , at different mass-damping parameter, δ_m , are computed and plotted in Fig. 6. It is noted that the tubes become unstable by buckling and the critical reduced cross flow velocity, U_r^* , increases with δ_m.

Stability of a square array of 4 tubes and a triangular array of 3 tubes, simply supported, are also studied. The results for these cases are presented in Fig. 7 and 8.

Tanaka and Takahara [24] experimentally measured the fluid forces coefficients for a row of tubes subjected to cross flow of water. These measured coefficients are not matching with the potential flow solution and also noted that these coefficients are dependent of cross flow velocity whereas those obtained from the potential flow theory are independent of cross flow velocity.

Chen [26] studied the published experimental data of critical cross flow velocity for various array of tubes. He observed that tubes were becoming unstable by flutter and not by buckling. Based on this collected informations, he gave the

Table 3. Added-mass Coefficients for a row of 5 tubes based on potential flow solution.

$$[\alpha_{ij}] = \begin{bmatrix} 1.113 & -0.282 & -0.282 & -0.04 & -0.04 \\ -0.282 & 1.112 & -0.037 & -0.287 & -0.017 \\ -0.282 & -0.037 & 1.112 & -0.017 & -0.287 \\ -0.04 & -0.287 & -0.017 & 1.058 & -0.011 \\ -0.04 & -0.017 & -0.287 & -0.011 & 1.058 \end{bmatrix}$$

$$[\sigma_{ij}] = [\tau_{ij}] = [0]$$

$$[\beta_{ij}] = \begin{bmatrix} 1.135 & 0.34 & 0.34 & 0.121 & 0.121 \\ 0.34 & 1.13 & 0.13 & 0.319 & 0.064 \\ 0.34 & 0.13 & 1.13 & 0.064 & 0.319 \\ 0.121 & 0.319 & 0.064 & 1.065 & 0.035 \\ 0.121 & 0.064 & 0.319 & 0.035 & 1.065 \end{bmatrix}$$

Table 4. : Fluid-damping coefficients for a row of 5 tubes based on potential flow solution.

$$[\alpha'_{ij}] = [\beta'_{ij}] = [0]$$

$$[\sigma'_{ij}] = \begin{bmatrix} 0.0 & 1.221 & -1.221 & 0.244 & -0.244 \\ -1.266 & -0.174 & -0.28 & 1.078 & -0.107 \\ 1.266 & 0.28 & 0.174 & 0.107 & -1.078 \\ -0.344 & -1.354 & -0.155 & -0.909 & -0.078 \\ 0.344 & 0.155 & 1.354 & 0.078 & 0.909 \end{bmatrix}$$

$$[\tau'_{ij}] = \begin{bmatrix} 0.0 & 0.974 & -0.974 & 0.04 & -0.04 \\ -0.93 & -0.134 & -0.032 & 0.98 & -0.008 \\ 0.93 & 0.032 & 0.134 & 0.008 & -0.98 \\ -0.003 & -0.741 & 0.006 & -0.426 & 0.005 \\ 0.003 & -0.006 & 0.741 & -0.005 & 0.426 \end{bmatrix}$$

Table 5.: Fluid-elastic coefficients for a row of 5 tubes based on potential flow solution.

$$[\alpha''_{ij}] = \begin{bmatrix} 5.752 & -2.6 & -2.59 & -0.281 & -0.281 \\ -2.591 & 5.356 & -0.265 & -2.4 & -0.098 \\ -2.6 & -0.266 & 5.354 & -0.098 & -2.391 \\ -0.28 & -2.393 & -0.098 & -2.84 & -0.06 \\ -0.281 & -0.098 & -2.401 & -0.06 & 2.831 \end{bmatrix}$$

$$[\sigma''_{ij}] = [\tau''_{ij}] = [0]$$

$$[\mu''_{ij}] = \begin{bmatrix} -3.03 & 1.507 & 1.507 & 0.007 & 0.007 \\ 1.508 & -2.802 & 0.014 & 1.278 & 0.0004 \\ 1.507 & 0.014 & -2.801 & 0.0004 & 1.278 \\ 0.007 & 1.286 & 0.0004 & -1.296 & 0.001 \\ 0.007 & 0.0004 & 1.286 & 0.001 & -1.295 \end{bmatrix}$$

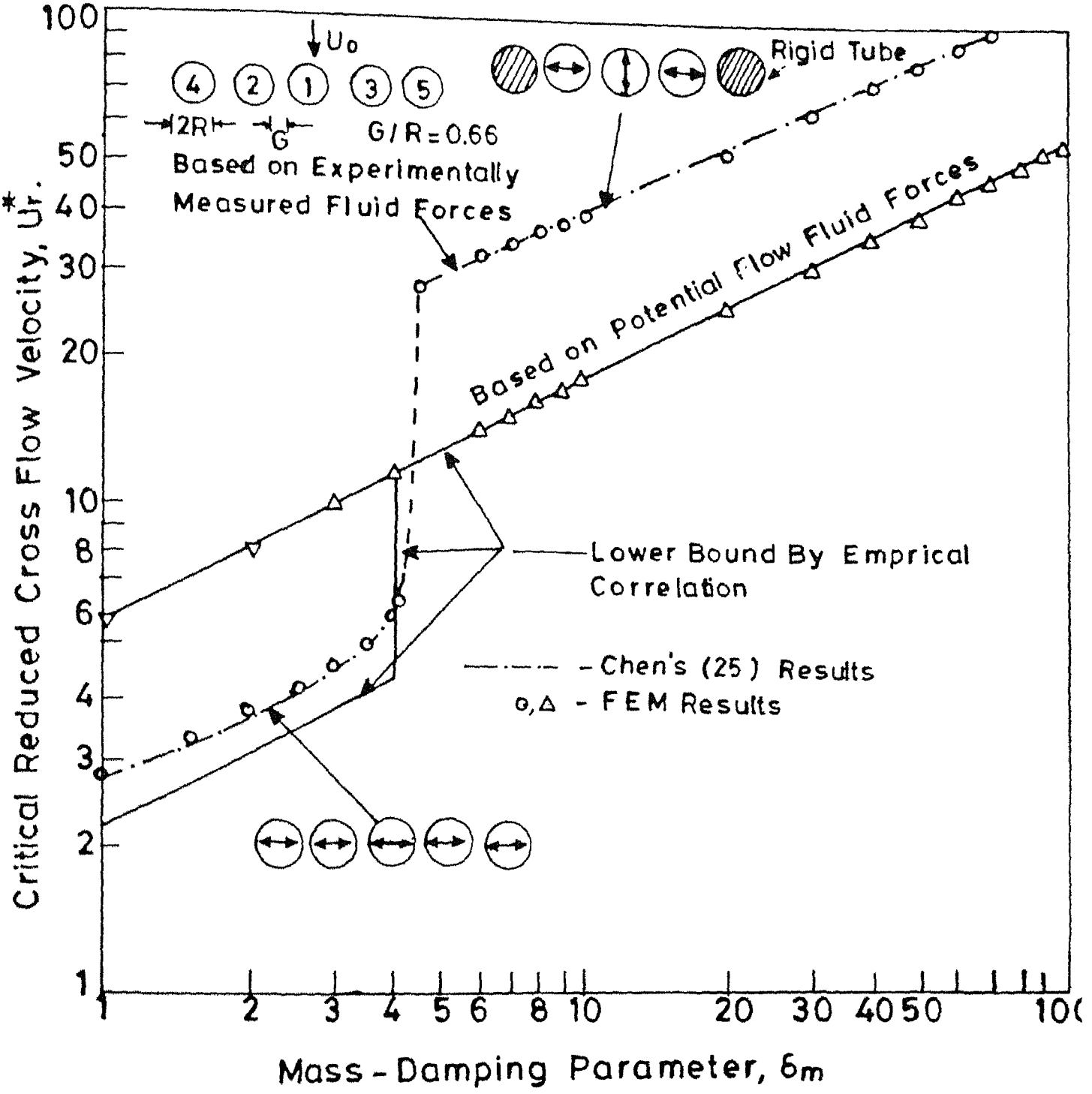

Fig.6 Critical Cross Flow Velocity U_r^*, for a Row of 5 Tubes in Cross Flow.

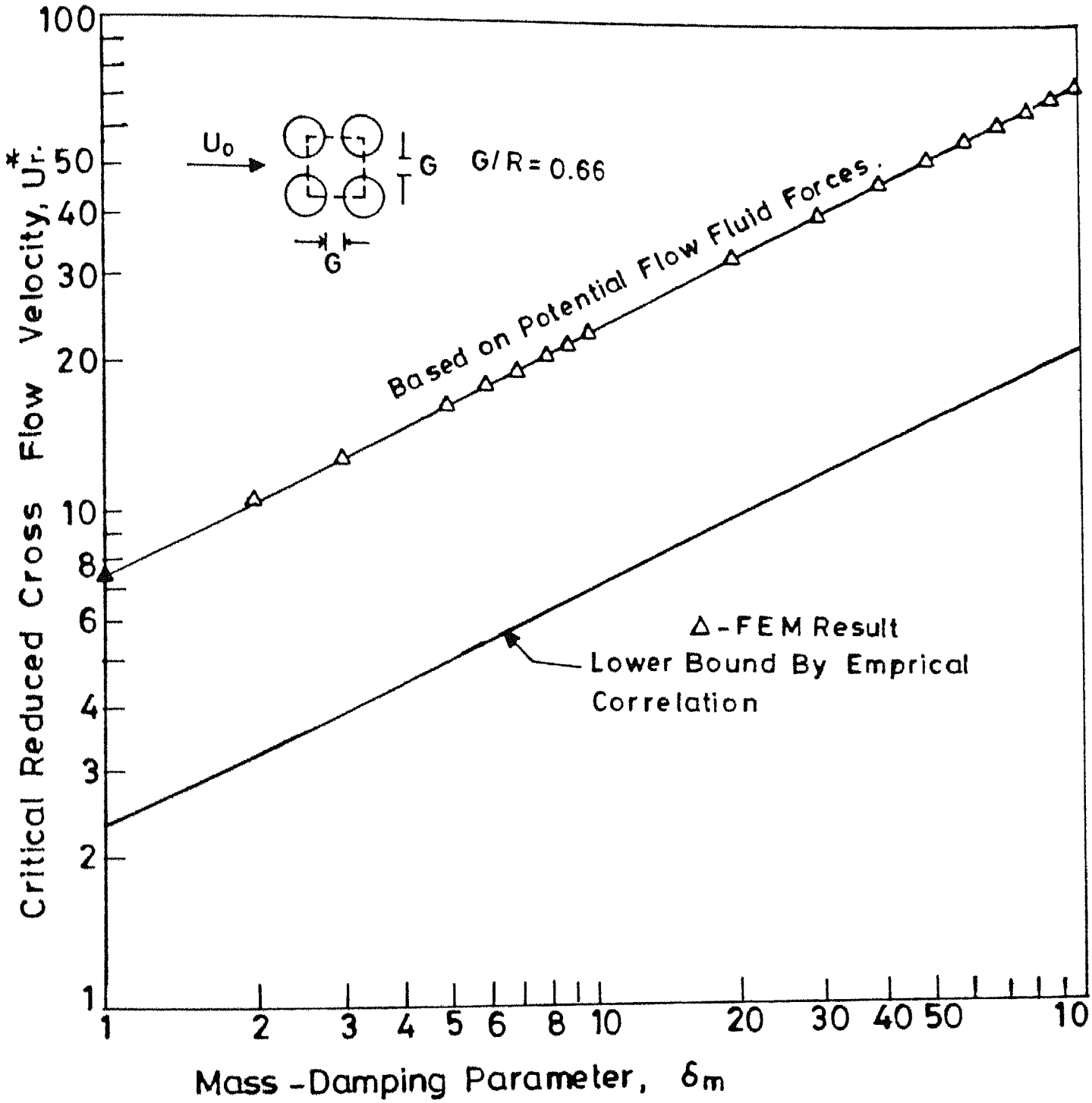

Fig. 7 Critical Cross Flow Velocity U_r^*, for a Square Array in Cross Flow.

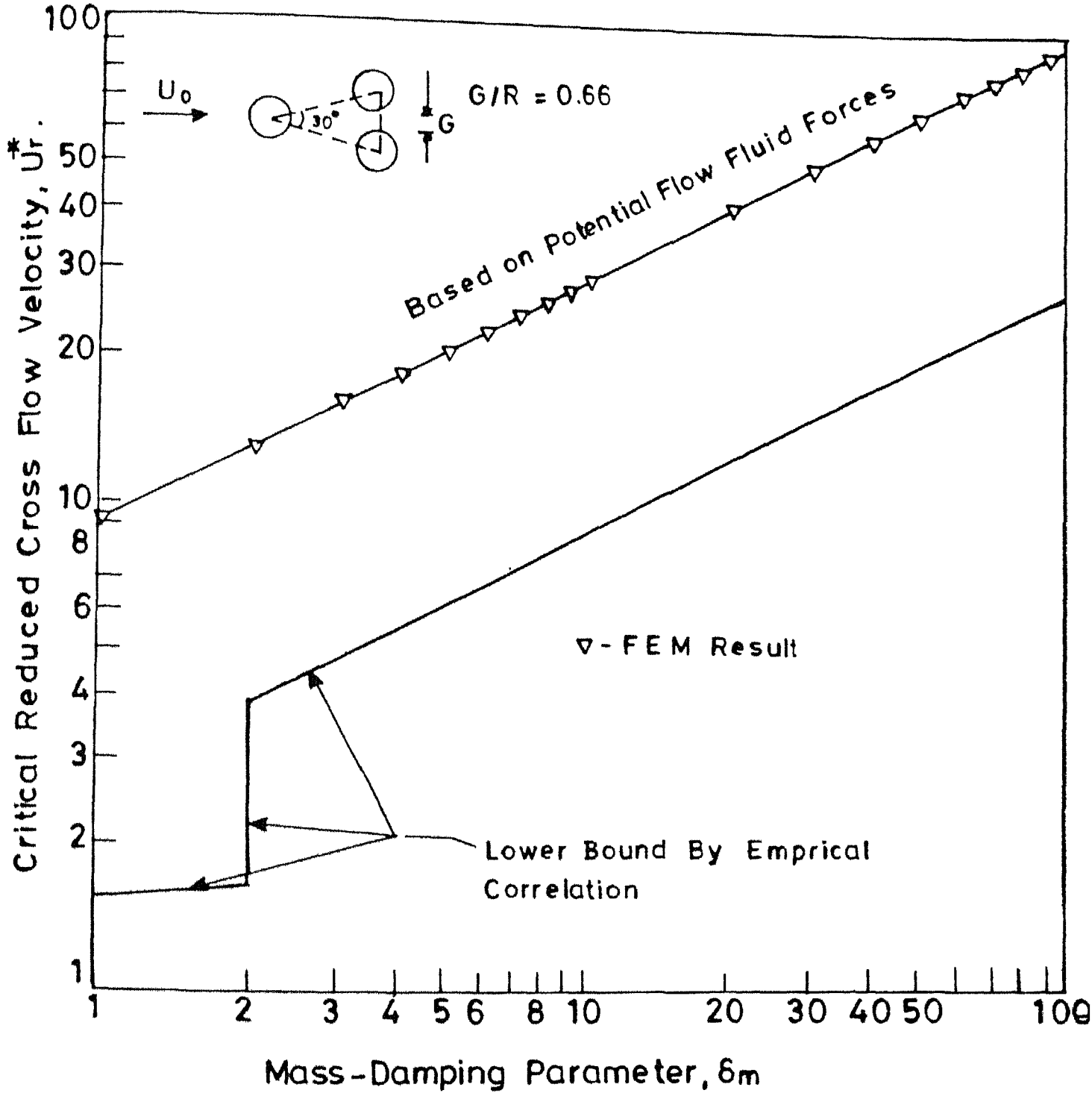

Fig.8 Critical Cross Flow Velocity U_r^*, for a Triangular Array in Cross Flow.

empirical correlations for the lower bound of critical reduced cross flow velocity, [26] . Using these correlations, the lower bound of critical reduced cross flow velocity for the above cases are plotted in Fig. 6 to 8.

Using the measured fluid force coefficients of Tanaka, Chen [25] studied the stability of a tube row. It was observed that there was dynamic instability of tubes. This can arise due to fluid damping or fluid-elastic forces. In case of fluid damping forces, energy transfer from cross flow to tubes is by tube velocities and the instability so caused is attributed to velocity mechanism and for fluid-elastic forces, energy transfer is by tube displacements and the instability so caused is attributed to displacement mechanism.

When cross flow velocity is small, the velocity of the tubes will be of the same order of the magnitude of the cross flow velocity, velocity mechanism causes the instability. Chen [25] found that this happens for $U_r < 15$ for a row of 5 tubes and experimental results showed that the tube oscillation are predominant in lift direction.

When cross flow velocity is large, fluid-elastic forces are dominant and displacement mechanism causes the instability. Chen [25] found that this instability can occur for $U_r > 15$ for a row of 5 tubes. For the row of 5 tubes, his experimental

results showed that the middle tubes oscillated predominately in the drag direction while the neighbouring tubes oscillated predominantely in the lift direction.

The critical reduced cross flow velocities, U_r^*, for a row of five tubes are calculated by FEM, using the measured coefficients of Tanaka [24] and model of Chen [25]. For $U_r < 15$, tubes were taken as vibrating in lift direction, and for $U_r > 15$, middle tube was taken as vibration in drag direction, next two in lift direction and last two as rigid, Chen [25] . He also neglected the fluid-damping force, fluid interia force and diagonal elements of the fluid-elastic force for $U_r > 15$. These results are shown in Fig. 6 and match well with those given by Chen [25] . It may be noted that if fluid-damping, fluid inertia and diagonal elements of the fluid-elastic forces were not neglected, the tube-row was found to be stable. For this row of 5 tubes, it is seen that dynamic instability is caused by velocity mechanism for $\delta_m < 4$ and by displacement mechanism for $\delta_m > 4.5$.

The critical reduced cross flow velocities, U_r^*, obtained by potential flow fluid forces and measured fluid forces differ widely. The mode of failure is buckling based on potential flow theory and dynamic instability based on measured fluid forces. It can be explained as follows.

Instability can arise due to fluid-elastic or fluid damping forces. Table 5 gives the potential flow solution of the fluid-elastic force matrix. In it, the diagonal sub-matrices $[\alpha'']$ and $[\beta'']$ are non-zero and off-diagonal sub-matrices $[\sigma'']$ and $[\tau'']$ are zero. From Eqn. (2.14) it is clear that buckling instability is controlled by $[\alpha'']$ and $[\beta'']$ matrices and dynamic instability by $[\sigma'']$ and $[\tau'']$ matrices. Thus as per potential flow theory, only buckling instability can occur.

Table 4 gives the potential flow solution of the fluid-damping force matrix. Diagonal sub-matrices $[\alpha']$ and $[\beta']$ are zero and off-diagonal sub-matrices $[\sigma']$ and $[\tau']$ are nonzero in it. From Eqn. (2.14), it is clear that the dynamic instability is controlled by $[\alpha']$ and $[\beta']$ matrices which are zero as per potential flow theory.

It clearly indicates that some of the assumptions made in calculating the fluid forces by potential flow theory are incorrect. As already mentioned, the tube movements are predominantely in lift direction for fluid-damping controlled instability. This phenomenon is similar to galloping of transmission lines. So the vortex shedding behind the tubes may be a source for this instability and the assumption of irrotational flow is incorrect.

In case of fluid-elastic controlled instability, the cross flow velocity is high. At this velocity, separation of flow is possible. Hence the assumption of no separation of flow is incorrect in finding the fluid forces by potential flow theory.

Leaver and Weaver [27] , noted that, when a tube moves from its equilibrium position, the stream lines of the flow will change but this redistribution will not take immediately. There is a phase lag for the distribution of flow due to fluid inertia. This point should be included in finding the fluid forces.

So the method of calculating the fluid forces needs a lot of improvement.

3.6 VIBRATION OF TUBE BANKS SUBJECTED TO THE COMBINED CROSS FLOW AND AXIAL INTERNAL FLOW :

In this section, the effect of axial internal flow, V, on the critical reduced cross flow velocity, U_r^* , is studied for a row of 5 tubes only. The fluid forces acting on the tube row due to cross flow are obtainable from the potential flow theory and experimentally measured data. Both of them have been used for this analysis. Below the critical axial flow velocity, V^*, only, the effect is studied (critical axial flow velocity, V^*, is one at which first instability occurs for a tube subjected to axial internal flow only). Because,above this axial internal flow velocity, the internal flow alone can cause the instability.

First,the row of five uniformly spaced simply-supported tubes based on potential flow theory is studied. The arrangements of the tubes and direction of flow are shown in Fig. 9. The gap to radius ratio, G/R, inside fluid mass ratio, β and damping ratio, τ, are taken as 0.66, 0.55 and 0.02 respectively. The results of

the critical reduced cross flow velocity, U_r^*, of the tube row are given in Fig. 9 as a function of mass-damping parameter, δ_m, for V=0, 2.0, 2.5. The critical reduced cross flow velocity, U_r^*, decreases with the increase in axial internal flow velocity, V. Fig. 10 shows, the critical reduced cross flow velocity, U_r^*, as a function of axial internal flow velocity, V, for δ_m= 1.0, 5.0, 50.0. From these figures, it is also noted that the effect on the critical reduced cross flow velocity is small for low axial flow velocity, V and it is large when it approaches the critical axial flow velocity, V^*. The fixed-fixed tube-row is also studied and the results are given in Fig. 11 and 12. Similar trends are observed in this case also.

With the experimentally measured fluid forces, the critical reduced cross flow velocities of simply-supported tube are also calculated and the results are given in Fig. 13 as a function of δ_m for V= 0.0, 2.0, 2.5. Fig. 14 shows the critical reduced cross flow velocity, U_r^*, as a function of axial internal flow velocity for δ_m = 1.0, 5.0, 50.0. From these figures it is noted that the axial internal flow velocity reduces the critical cross flow velocity in the region of U_r > 15. This can be explained as follows. Paidoussis [3] showed for a simply-supported pipe with internal flow, the frequency decreases with axial flow velocity and becomes zero at critical velocity (π) and buckles.

This shows that stiffness goes on decreasing with increase in velocity and damping has no effect. Thus internal flow has effect in the fluid-elastic controlled instability region $U_r > 15$. Fixed-Fixed tubes are also studied and the results are shown in Fig. 15 and 16. Similar trends are also observed in this case.

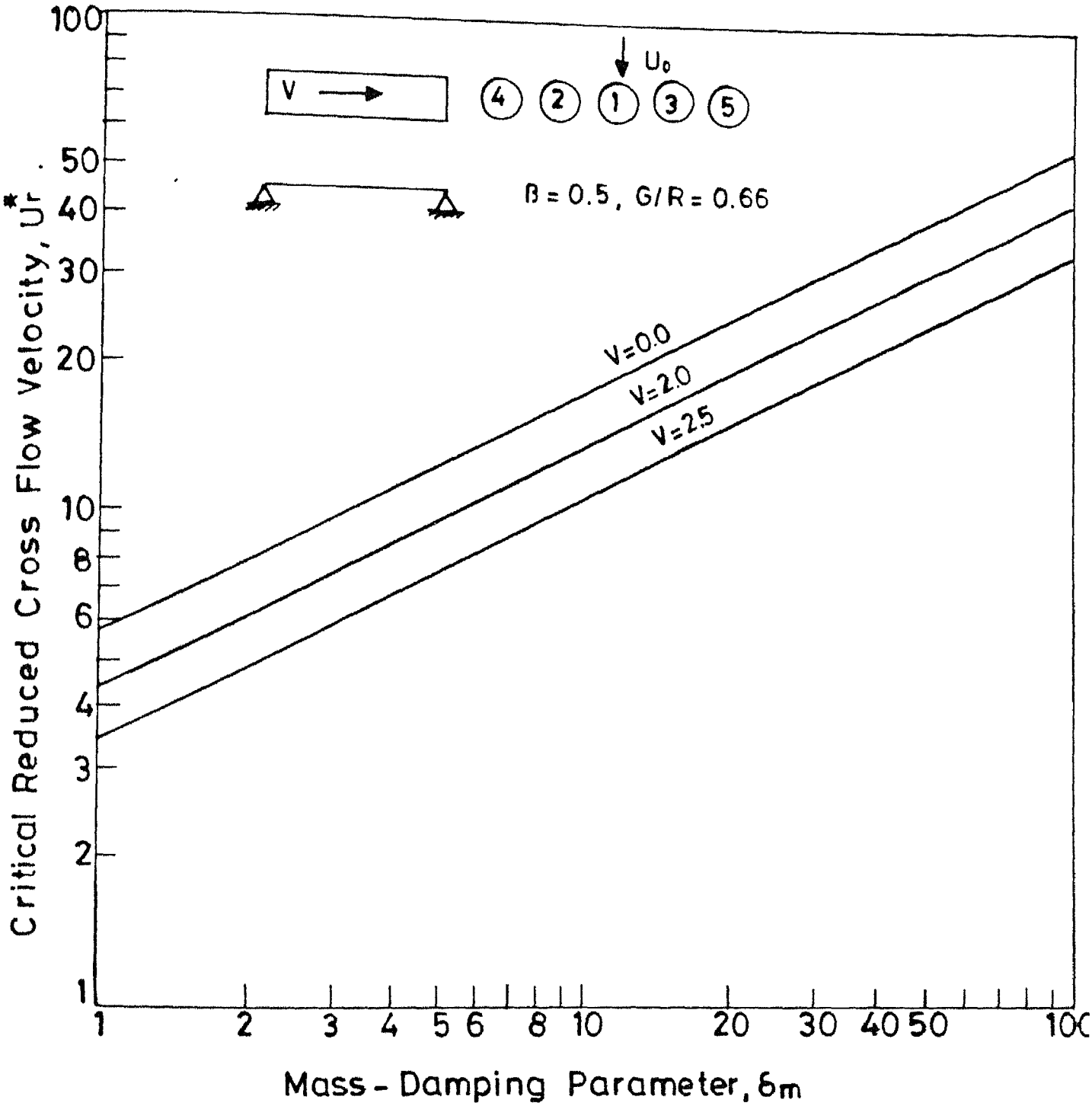

Fig.9 Critical Cross Flow Velocity U_r^* as a Function of δ_m for a Row of 5 Simply - Supported Tubes Subjected to the Combined Flows (Based on Potential Flow Fluid Forces.)

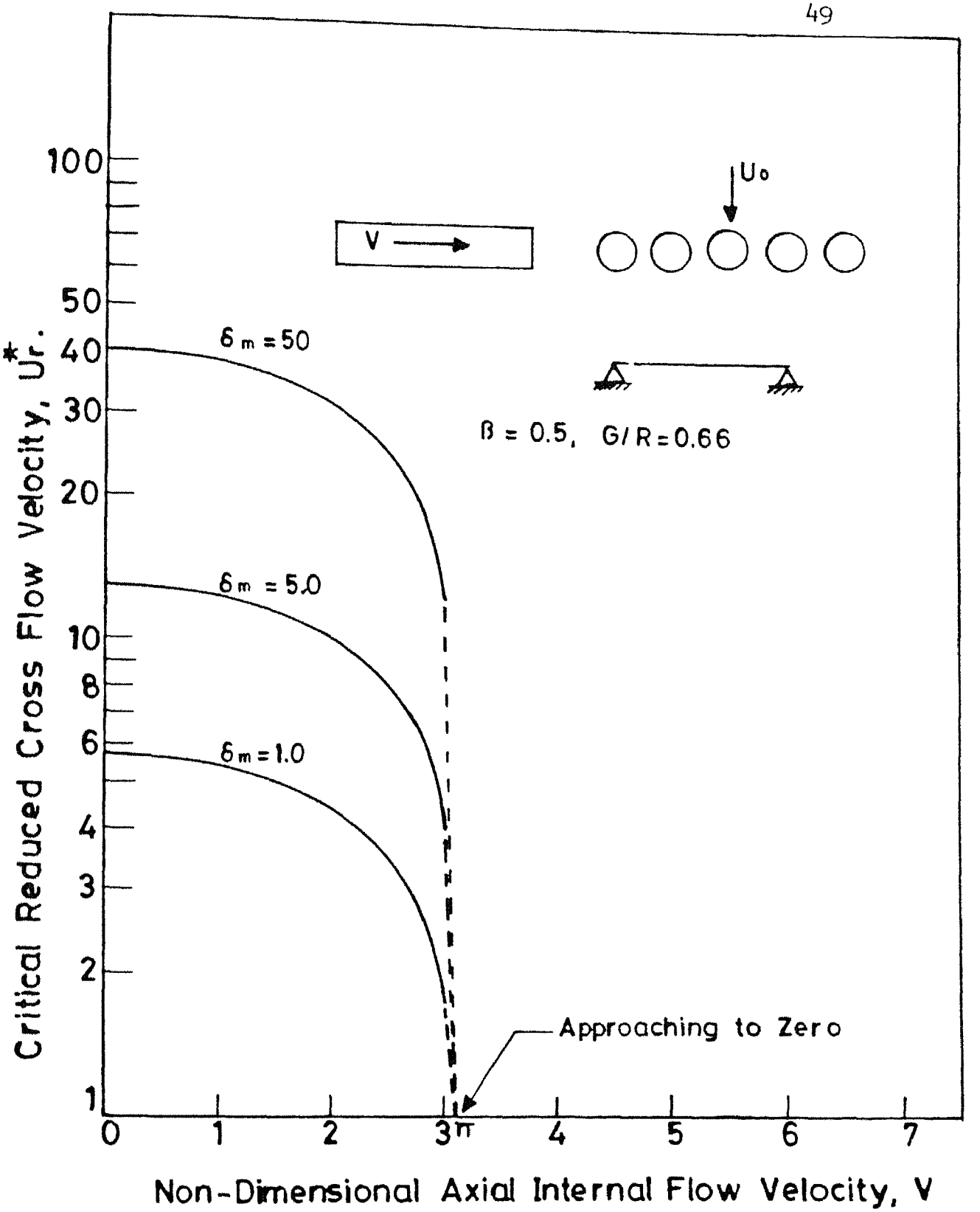

Fig.10 Critical Cross Flow Velocity, U_r^*, as a Function of V for a Row of 5 Simply-Supported Tubes Subjected to the Combined Flows (Based on Potential Flow

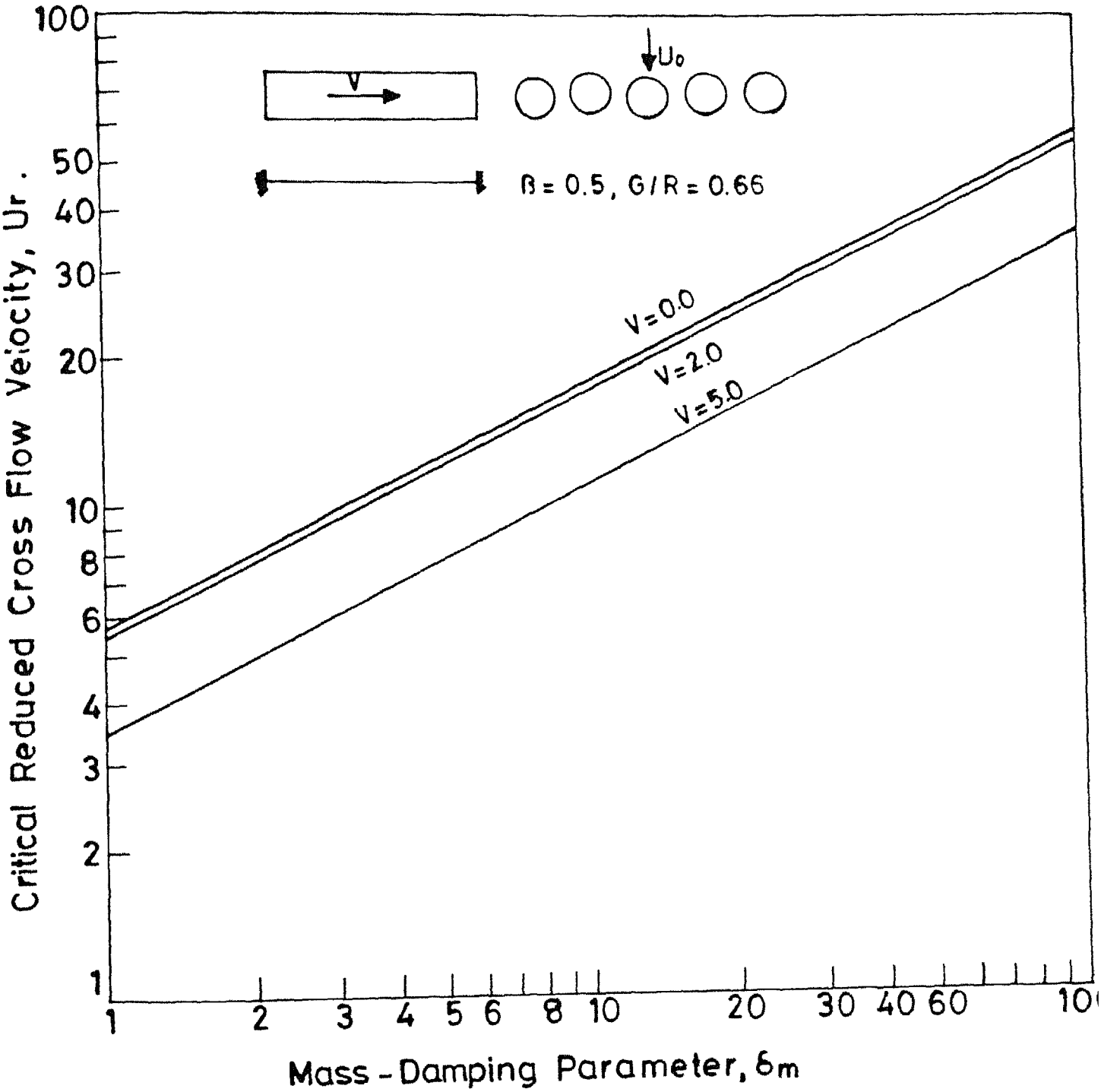

Fig.11 Critical Cross Flow Velocity U_r^*, as a Function of δ_m for a Row of 5 Fixed - Fixed Tubes Subjected to the Combined Flows (Based on Potential Flow Fluid Forces.)

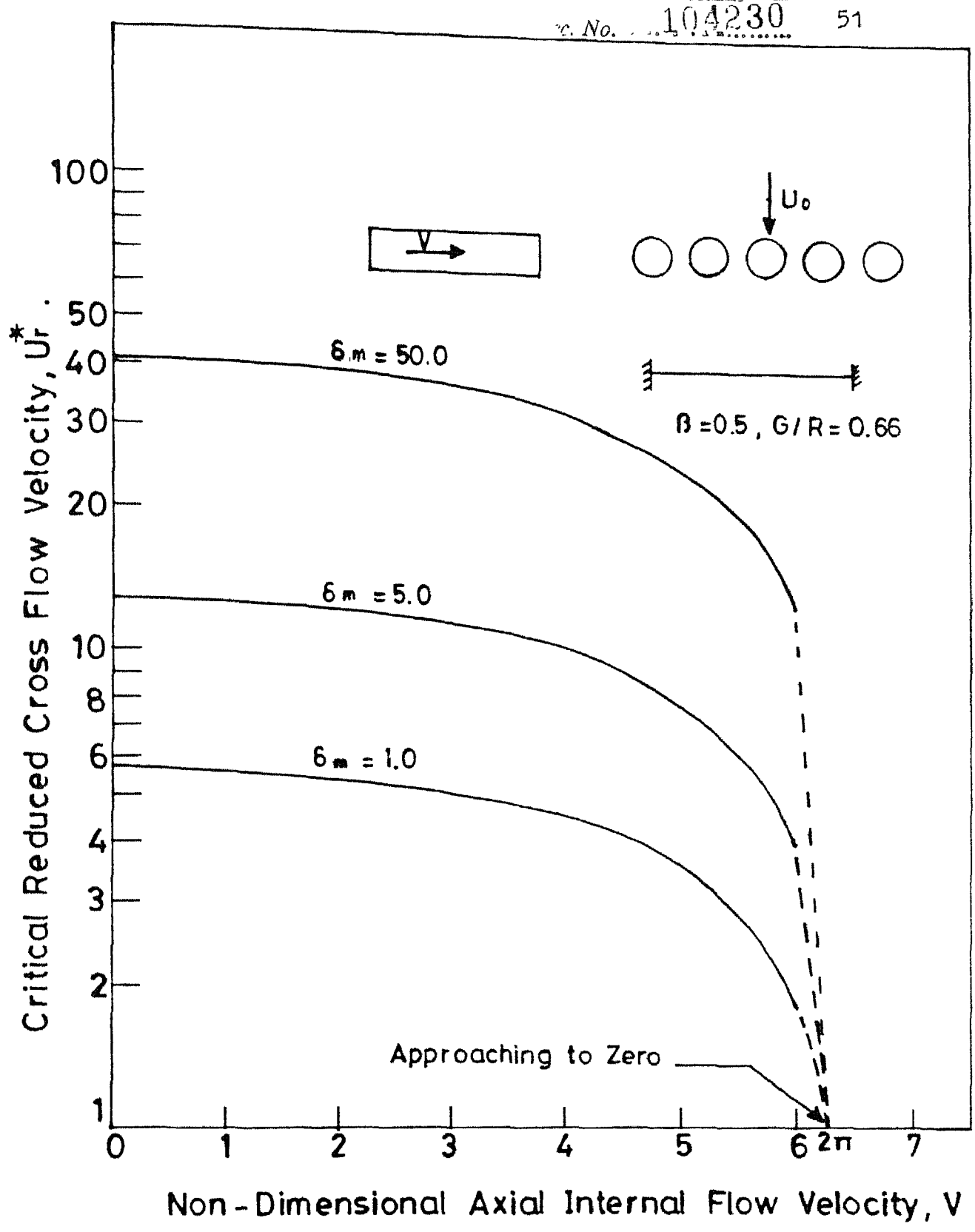

Fig.12 Critical Cross Flow Velocity U_r^*, as a Function of V for a Row of 5 Fixed-Fixed Tubes Subjected to the Combined Flows (Based on Potential Flow Fluid Forces)

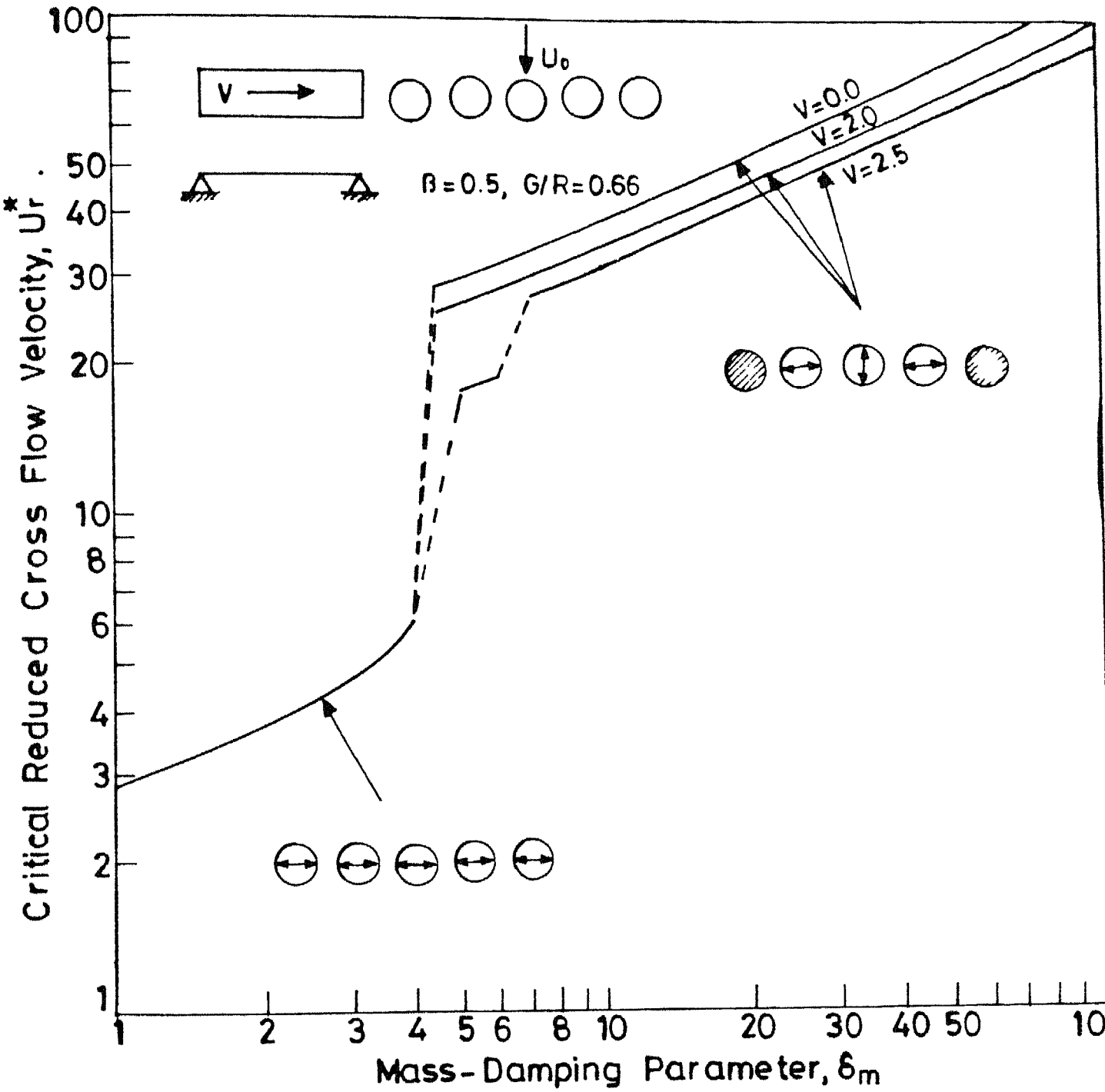

Fig.13 Critical Cross Flow Velocity, U_r^*, as a Function of δ_m for a Row of 5 Simply-Supported Tubes Subjected to the Combined Flows (Based on Experimentally Measured Fluid Forces)

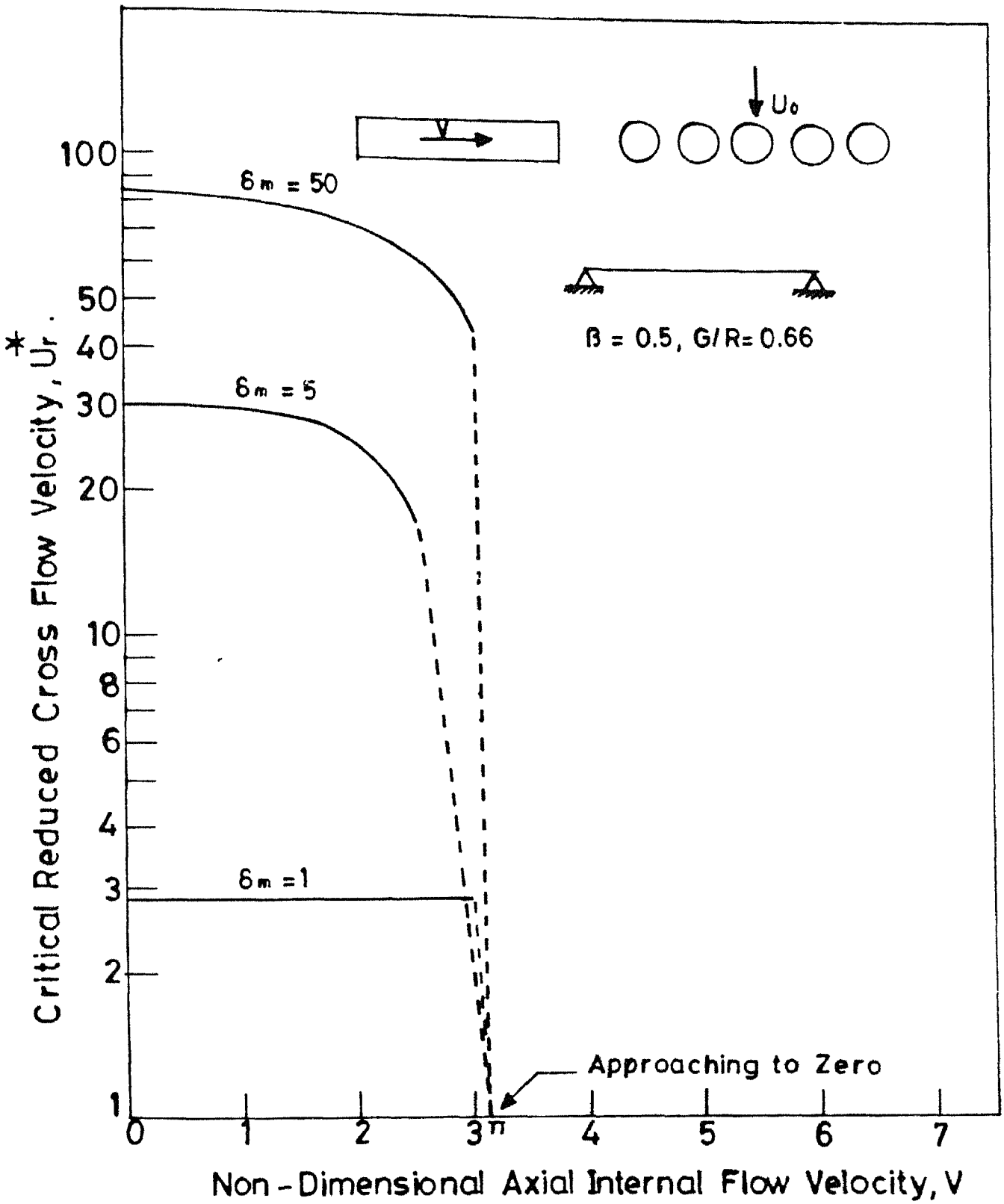

Fig. 14 Critical Cross Flow Velocity U_r^*, as a Function of V for a Row of 5 Simply-Supported Tubes Subjected to the Combined Flows (Based on Experimentally Measured Fluid Forces.)

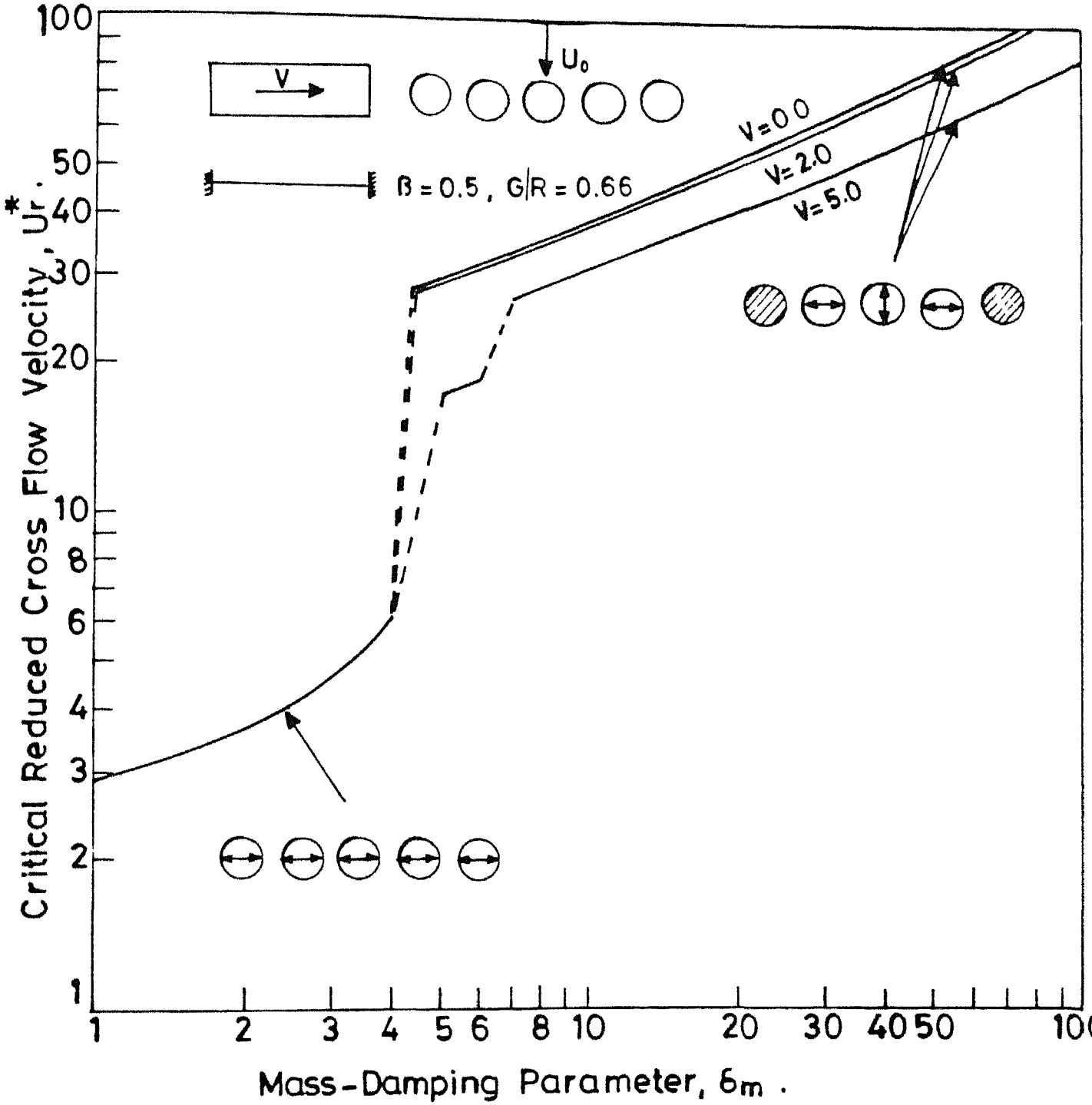

Fig. 15 Critical Cross Flow Velocity U_r^* as a Function of δ_m for a Row of 5 Fixed-Fixed Tubes Subjected to the Combined Flows (Based on Experimentally Measured Fluid Forces.)

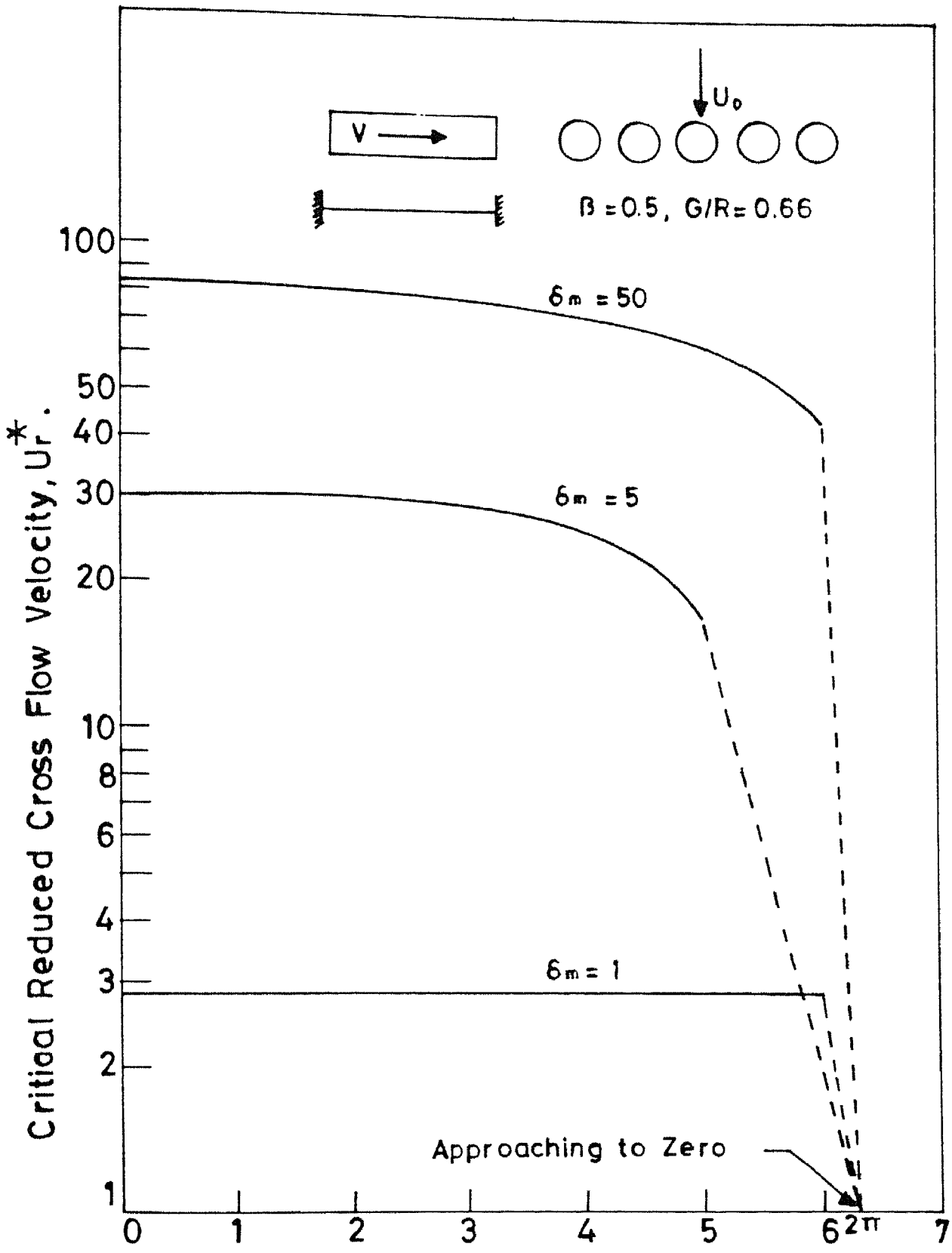

Fig.16 Critical Cross Flow Velocity U_r^*, as a Function of V for a Row of 5 Fixed-Fixed Tubes Subjected to the Combined Flows (Based on Experimentally Measured Fluid Forces.)

CHAPTER-IV

CONCLUSIONS

In the present work, the equations of motion of a tube bank vibrating in the combined cross and axial internal flow have been derived. These equations are transfermed into a set of simultaneous ordinary differential equations, using FEM. From these equations, results are obtained for tube banks in

(i) stationary outside fluid,

(ii) cross flow and

(iii)combined cross and axial internal flow.

for some of the parameters like outside fluid mass ratio, gap to radius ratio and number of tubes with different configuration. Based on these results and discussions presented in Chapter III, the following conclusion are arrived at

1. The improved mathematical model for analysing combined cross and axial internal flow is a general one. This model has been used for analysing the tube banks in (a) stationar outside fluid, (b) cross flow and (c) combined cross and axial internal flow.

2. The finite element solution for the vibration of simply-supported tube-row vibrating in stationary outside fluid agrees well that of closed form solution by Chen [20], which validates the FEM formulation developed in this work.

3. In cross flow, the results obtained by the fluid forces of potential flow theory are unrealistic. Hence the potential flow theory is unacceptable for finding the fluid forces in cross flow. Further improvements are needed in finding these forces by analytical.

4. Results obtained for the combined cross and axial internal flow of the simply-supported and fixed-fixed tube-row, using measured fluid forces, indicate that the axial flow velocity reduces the critical cross flow velocity in the fluid-elastic controlled instability region ($U_r > 15$ and $\delta_m > 4.5$).

There is a considerable scope of research being conducted in the combined cross and axial internal flow induced vibration in particular the mechanism associated with the onset of instabilities.

REFERENCES

1. Paidoussis, M.P., "Flow-Induced Vibrations in Nuclear Reactors and Heat-Exchangers: Practical Experience and State of Knowledge", Practical Experience with Flow-Induced Vibrations, eds. E. Naudascher and D. Rockwell, Springer-Verlag Berlin, 1980, pp. 1-81.

2. Blevins, R.D., "Flow-Induced Vibration", Von-Nostrand Rheinhold Co., New York, 1977.

3. Paidoussis, M.P., and Issid, N.T., "Dynamic Stability of Pipes Conveying Fluid", Journal of Sound and Vibration, Vol. 33, 1974, pp. 227-294.

4. Chen, S.S., "Parallel Flow-Induced Vibrations and Instability of Cylinderical Structures", The Shock and Vibration Digest, Vol. 6, No. 10, 1974, pp. 1-11.

5. Housner, G.W., "Bending Vibration of a Pipeline Containing Flowing Fluid", ASME, Journal of Applied Mechanics, Vol. 19, 1952, pp. 205-298.

6. Gregory, R.W., and Paidoussis, M.P., "Unstable Oscillation of Tubular Contilevers Conveying Fluid ; Part I : Theory, Part II: Experiments", Proceedings of Royal Society of London, A, Vol. 293, 1966, pp. 512-527 and 528-542.

7. Naguleswaran, S., and Williams, C.J.W., "Lateral Vibration of Pipe Conveying Fluid", Journal of Mechanical Engg. Science, Vol. 10, No.3, 1968, pp. 228-238.

8. Chen, S.S., "Flow-Induced Vibration of an Elastic tube", The ASME Presentation at the Vibration Conference and the International Design Automation Conference, Sept. 8-10,1971.

9. Deb, J.K.," Dynamic Stability of Pipes Conveying Fluid by Finite Element Method", M.Tech. Thesis, Dept. of Mechanical Engineering, IIT.,Kanpur,1978.

10. Ravi Kumar," Dynamic Stability of Multi-Span Pipes Conveying Fluid by Finite Element Method", M.Tech. Thesis, Dept. of Mechanical Engineering, IIT., Kanpur, 1982.

11. Debasis Mishra," Flow-Induced In-Plane and Out-of-Plane Vibration and Stability of Stright, Curved and U-Bend Timoshenko Tubes by FEM", M.Tech. Thesis, Dept. of Mechanical Engg., IIT., Kanpur,1987.

12. To, C.W.S., and Kaladi, V.," Vibration of Pipe Systems Containing a Moving Medium", Journal of Pressure Vessel Technology , Vol. 107, 1986. pp. 344-349.

13. Shin, Y.S., and Wambsganss, M.W., "Flow Induced Vibration in LMFBR Steam Generator : A State of the Art-Review", Nuclear Engg. and Design, Vol. 40, No.2, 1977, pp. 235-284.

14. Chen, S.S.," Flow Induced Vibrations of Circular Cylinderical Structures ; Part I : Stationary Fluids and Parallel Flow, Part II: Cross Flow Considerations", Shock and Vibration Digest, Vol. 9, 1977, No. 10, pp. 25-38, No. 11, pp. 21-27.

22. Ho, Chung and Chen, S.S.," Vibration of a Group of Circular Cylinder in a Confined Fluid", Journal of Applied Mechanics, 1977, 213-217.

23. Chen, S.S., "Cross Flow Induced Vibrations of Heat Exchanger Tube Banks", Nuclear Engg . and Design, Vol. 47, 1978, pp. 67-86.

24. Tanaka, H., and Takahara, S., "Unsteady Fluid Force on Tube Bundle and its Dyramic Effect on Vibration", Flow-Induced Vibration of Power Plant Components, eds., Au-Yang, M.K., ASME, New York, 1980.

25. Chen, S.S., " Instability Mechanism and Stability Criteria of a Group of Circular Cylinders Subjected to Cross Flow ; Part I : Theory, Part II : Numerical Results and Discussions Journal of Vibration, Acoustics, Stress and Reliability in Design, Vol. 105, 1983, pp. 51-58, pp. 253-260.

26. Chen, S.S., "The Instability Flow Velocity of Tube Array in Cross Flow", International Conference on Flow Induced Vibration in Fluid Engg., England, Sep. 14-16, 1982.

27. Lever, J.H., andWeaver, D.S.,"A Theoretical Model for Fluid-Elastic Instability in Heat-Exchanger Tube Bundles", Journal of Pressure Vessel Technology, Vol. 104, 1982, pp. 147-158.

28. "Flow-Induced Structural Vibrations", ed. E. Naudascher, Spring-Verlag, Berlin, 1974.

29. "Flow-Induced Vibrations", eds., Chen, S.S., Martin D. Bernstein, ASME, The Third National Congress on Pressure Vessel and Piping Technology, San Francisco, California, June 25-29, 1979.

30. "Practical Experience with Flow-Induced Vibrations" , eds., E. Naudascher, and D. Rockwell, Springer-Verlag, Berlin, 1980.

31. "Internation Conference on Flow-Induced Vibrations in Fluid Engineering", England, Sep. 1982.

32. Meirovitch, L., "Analytical Methods in Vibrations", The Macmillan Company, London, 1967, p. 410.

33. Frazer, R.A., Duncan, W.J. and Collar, A.R., "Elementry Matrices", Cambridge University Press, New York, 1957, p. 327.

.....	.....
.....	.....
.....	.....
.....	.....
.....	.....
.....	.....
.....	.....
.....	.....
.....	.....
.....	.....
.....	.....